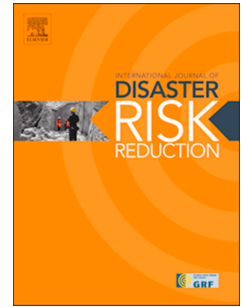# Journal Pre-proof

Scoring, selecting, and developing physical impact models for multi-hazard risk assessment

Roberto Gentile, Gemma Cremen, Carmine Galasso, Luke T. Jenkins, Vibek Manandhar, Emin Yahya Mentese, Ramesh Guragain, John McCloskey

Please cite this article as: R. Gentile, G. Cremen, C. Galasso, L.T. Jenkins, V. Manandhar, E.Y. Mentese, R. Guragain, J. McCloskey, Scoring, selecting, and developing physical impact models for multi-hazard risk assessment, *International Journal of Disaster Risk Reduction* (2022), doi: https://doi.org/10.1016/j.ijdrr.2022.103365.

This is a PDF file of an article that has undergone enhancements after acceptance, such as the addition of a cover page and metadata, and formatting for readability, but it is not yet the definitive version of record. This version will undergo additional copyediting, typesetting and review before it is published in its final form, but we are providing this version to give early visibility of the article. Please note that, during the production process, errors may be discovered which could affect the content, and all legal disclaimers that apply to the journal pertain.

Scoring, selecting, and developing physical impact models for multi-hazard risk assessment

Roberto Gentile[1], Gemma Cremen[2], Carmine Galasso[2], Luke T. Jenkins[3], Vibek Manandhar[4], Emin Yahya Mentese[5], Ramesh Guragain[4], John McCloskey[6]

[1] Institute for Risk and Disaster Reduction, University College London, London, United Kingdom

[2] Department of Civil, Environmental and Geomatic Engineering, University College London, London, United Kingdom

[3] School of Earth Sciences, University of Bristol, Bristol, United Kingdom

[4] National Society for Earthquake Technology, Sainbu Awas, Nepal

[5] Kandilli Observatory and Earthquake Research Institute, Boğaziçi University, Istanbul, Turkey

[6] School of Geosciences, University of Edinburgh, Edinburgh, United Kingdom

Correspondence to: Roberto Gentile (r.gentile@ucl.ac.uk)

Abstract. This study focuses on scoring, selecting, and developing physical fragility (i.e., the probability of reaching or exceeding a certain DS given a specific hazard intensity) and/or vulnerability (i.e., the probability of impact given a specific hazard intensity) models for assets, with particular emphasis on buildings. Given a set of multiple relevant hazards for a selected case-study region, the proposed procedure involves 1) mapping the relevant asset classes (i.e., construction types for a given occupancy) in the region to a set of existing candidate fragility, vulnerability and/or damage-to-impact models, also accounting for specific modelling requirements (e.g., time dependency due to ageing/deterioration of buildings, multi-hazard interactions); 2) scoring the candidate models according to relevant criteria to select the most suitable ones for a given application; or 3) using state-of-the-art numerical or empirical methods to develop fragility/vulnerability models not already available. The approach is demonstrated for the buildings of the virtual urban testbed "Tomorrowville", considering earthquakes, floods, and debris flows as case-study hazards.

1. Introduction and motivation

Natural-hazard-induced disaster risk results from complex interactions between exposure, hazard, and vulnerability. According to widely accepted definitions (e.g., United Nations Office for Disaster Risk Reduction, UNDRR [1]), a hazard is "a process, phenomenon or human activity that may cause loss of life, injury or other health impacts, property damage, social and economic disruption or environmental degradation"; exposure is "the situation of people, infrastructure, housing, production capacities and other tangible human assets located in hazard-prone areas"; and vulnerability is referred to as "the conditions determined by physical, social, economic and environmental factors or processes which increase the susceptibility of an individual, a community, asset or system to the impacts of hazards". This paper specifically focuses on the physical vulnerability component of (multiple) natural-hazard disaster risk. The paper discusses the appraisal, scoring, selection, and development of models - collectively referred to as "physical impact models" (see Section 2 for more details) - that broadly quantify the consequences of a set of hazard intensity measures (IMs) on physical assets (e.g., buildings, infrastructure). Systemic vulnerability (e.g., [2]), originating from the mutual linkages/interactions among physical, economic, and social systems, is outside the scope of this paper. Furthermore, specific emphasis is placed on buildings, which act as critical nodes in modelling interacting physical infrastructure systems and social networks (e.g., [3,4]).

Detailed information on individual physical assets within a given region of interest may not always be available due to a lack of specific data (particularly in Global South contexts) required to infer (select) or derive appropriate asset-specific exposure models. In addition, for forward-looking risk analyses that focus on possible future configurations of an urban system (e.g., [5,6]), asset-by-asset information is not necessarily considered within the underlying procedures (e.g., urban planning) or

modelling (e.g., spontaneous urban growth prediction). Therefore, for vulnerability characterisation purposes, assets are generally grouped into classes based on a set of common attributes that define their exposure. These attributes uniquely describe an asset class (e.g., buildings, bridges, lifeline equipment), detailing the common features directly associated with the physical impacts of multiple natural hazards. Then, each class is assigned relevant fragility (i.e., the probability of reaching or
5   exceeding a certain DS, given a prescribed magnitude of a hazard IM) or vulnerability (i.e., the probability of impact given a prescribed magnitude of a hazard IM) models, which may account for single or multiple hazards. Vulnerability models may be linked to fragility models using appropriate damage-to-impact (i.e., the probability of impact given a certain DS) models. Each component of disaster risk may involve temporal dependence. Time-dependent fragility/vulnerability is herein defined as a variation over time of the parameters of the physical impact model for a given asset class definition (e.g., ageing of the
10 asset materials increases fragility over time but does not change the considered asset class). Moreover, fragility/vulnerability may change due to environmental asset deterioration (e.g., corrosion of structural components), the effects of sequential hazard events (e.g., damage accumulation due to multiple earthquake aftershock occurrences), or structural strengthening efforts (e.g., structural retrofit, climate adaptation engineering [7]). For accurate risk estimations, capturing the above dynamic effects is crucial (e.g., [8]).
15 Many fragility/vulnerability models are available for different combinations of asset types and hazards (single or multiple) within various sources, including literature review studies, compendia, and interactive online databases. However, selecting the most suitable models for a given asset class within a specific geographical context is a significant challenge for risk modellers or other end-users, particularly in forward-looking contexts such as risk-informed urban planning and future urban development. Different choices of physical impact models may lead to remarkably different risk estimates, which can affect
20 decision making based on these estimates. This paper provides a structured methodology for scoring, selecting, and developing multi-hazard physical fragility/vulnerability models of asset classes (with greater emphasis on buildings) within any selected case-study region in support of multi-hazard risk modelling and quantification. The process consists of three main steps: 1) mapping the relevant asset classes in a considered area to a set of existing candidate physical impact models, also accounting for specific modelling requirements (e.g., time dependency, multi-hazard interaction); 2) scoring the candidate models
25 according to relevant criteria, to select the most suitable models for a given application; or 3) using state-of-the-art empirical or synthetic (analytical or numerical) methods to develop fragility/vulnerability models not already available.
The paper is organised as follows. Section 2 introduces the types of physical impact models considered as part of the proposed methodology and discusses them in the context of a selection of natural hazard types. After describing it (in Section 3), the proposed procedure is then demonstrated (Section 4) for the virtual urban testbed "Tomorrowville" [9], which reflects typical
30 (and dynamic) demographic, socioeconomic and physical features of urban landscapes in the Global South. Tomorrowville is designed as a demonstration of the Tomorrow's Cities Decision Support Environment (TCDSE; [3], [10]), which is a framework that brings different actors together to envision possible futures of a city and facilitates multi-hazard risk-informed urban planning, design, and development accordingly [11]. The illustrative application of this paper directly relates to the "Physical Infrastructure Impact" module of the TCDSE as applied to Tomorrowville, considering earthquakes, floods, and
35 debris flows as case-study hazards. A detailed description of physics-based hazard modelling for Tomorrowville is discussed in [12].

2. Overview of physical impact models for natural hazards

This Section introduces the types of physical impact models (i.e., fragility relationships, vulnerability relationships, damage-to-impact models) that form the basis of the scoring/selection/development methodology proposed in Section 3. These models
40 may be empirical, synthetic, or expert elicitation based. Empirical physical impact models require collecting data related to previous observations of natural-hazard (post-event) physical impacts (damage and/or consequences). Synthetic physical impact models are derived from analytical or numerical modelling of an asset's "response" (e.g., structural and/or nonstructural) to one or more hazards of interest, which is linked to physical damage and consequence metrics of interest. Expert-elicitation models involve several experts providing educated guesses of the damage (or consequence) that would occur
45 to a specific asset class when subjected to a prescribed magnitude of a hazard IM. Each model type may be derived based on asset-level damage and/or impact data (i.e., global-level analysis) or damage and/or impact data for each component of the considered asset (i.e., component-by-component analysis) aggregated to obtain asset-level results. Empirical and expert-

elicitation physical impact models are usually derived from a global-level analysis, while synthetic models can be based on either global or component-by-component analyses.

This Section begins with the mathematical definitions of these models and then provides a brief overview of their implementation for selected natural-hazard contexts, including the relevant damage causes or mechanisms, adopted IMs, and
5   other pertinent information on how the different physical impact model types are structured.

2.1. Mathematical definitions

2.1.1. Fragility relationships

Asset-level fragility relationships define the probability of some discrete limit (or damage) state (DS_i) being reached or exceeded for an asset of interest, as a function of hazard intensity, i.e., $P(DS \geq ds_i|IM = im)$. (Note that lower-case symbols
10   refer to a particular value of the random variables denoted in upper case). The response of an asset to a hazard-induced loading (e.g., earthquake-induced ground-motion time history, flood-induced hydrostatic/hydrodynamic forces, etc.) described by a certain IM is quantified using an engineering demand parameter (EDP, e.g., building horizontal roof displacement, floor accelerations, the stress level in a given structural component). The selected IM for the analysis should be both efficient and sufficient (e.g., [13]). An efficient IM leads to a relatively small variability in estimating the selected EDP given a prescribed
15   value of IM. A sufficient IM renders the estimation of the EDP for all IM levels independent of all other hazard causal parameters (e.g., earthquake magnitude and location). Fragility relationships can also be represented using vector-valued IMs (as described in Section 2.1.4).

Fragility functions typically take the form of lognormal cumulative distribution functions (CDFs e.g., [14,15]):

$$P(DS \geq ds_i|IM = im) = \Phi\left(\frac{\ln\left(\frac{im}{\theta}\right)}{\beta}\right), \qquad 1$$

where $\Phi(\cdot)$ is the standard normal CDF, θ is the median (i.e., the value of IM that results in a 50% probability of reaching or
20   exceeding ds_i), and β is the standard deviation of $\ln(IM)$ for ds_i. This mathematical form has several features that are particularly convenient in the context of fragility modelling fragility, including the exclusion of non-plausible negative IM values and the fact that the θ and β parameters are enough to define the function completely. An extensive description of other potential mathematical forms that can describe fragility is provided in [16,17], among many others. Both Lallemant et al. [17] and Jalayer et al. [18] also discuss the possibility of updating fragility functions (if more information – from experimental
25   results or post-event fieldwork, for instance – subsequently becomes known) using Bayesian methods. A more advanced fragility function model, which explicitly accounts for the ordinality of damage (i.e., the fact that DSs are both ordered and related in a physical sense) through simultaneous calibration of functions for multiple DSs, was recently presented in [19].

2.1.2. Vulnerability relationships

Vulnerability relationships are used to estimate the probability of continuous outcomes (O) – typically in the form of an impact
30   (or consequence) metric (e.g., economic losses, downtime, casualties) – associated with a given IM, i.e., $P(O>o|IM=im)$. Vulnerability functions that produce absolute values of outcomes are generally expressed in the form:

$$P(O > o|IM = im) = 1 - F(o|im), \qquad 2$$

where $F(.)$ is some type of CDF. Vulnerability functions that output relative values of outcome (e.g., economic loss normalised with respect to the asset value) can take the form of a Beta distribution, given its ability to flexibly model values between 0 and 1 [20,21]. In this case,

$$f(o|IM = im) = \frac{o^{q-1}(1-o)^{r-1}}{B(q,r)} \qquad 3$$

35   where r and q specify the shape of the distribution, and $B(.)$ denotes the beta function.

Vulnerability models often neglect uncertainty in the outcome, simply estimating the mean (absolute or relative) value of an outcome conditional on IM, i.e., $E(O|IM = im)$. These functions are typically derived using some form of regression curve/surface [22–25].

3

2.1.3. Damage-to-impact models

Damage-to-impact models – often referred to as consequence or damage-to-loss models – bridge the gap between fragility and vulnerability analysis in the absence of appropriate parametric vulnerability relationships, by mapping discrete DSs to continuous impact metrics [26]. Probabilistic versions of these models take the form $P(O > o|DS = ds_i)$, and can be used to derive a vulnerability function through:

$$P(O > o|IM = im) = \sum_{i=1}^{n} P(O > o|DS = ds_i)P(DS = ds_i|IM = im) \qquad 4$$

where $P(DS = ds_i|IM = im) = P(DS \geq ds_{i-1}| IM = im) - P(DS \geq ds_i| IM = im)$, n denotes the number of DSs, and all other variables and expressions are as previously defined. Given the similar mathematical forms of vulnerability and damage-to-impact models, the Beta distribution can also be used to model $f(o|ds_i)$, e.g., [27]. Deterministic damage-to-impact models - expressed as $E(O|DS = ds_i)$ - translate $P(DS = ds_i|IM = im)$ into $E(O|IM = im)$ through an analogue form of Eq. 4. (e.g., [28]).

2.1.4. Extensions to multi-hazard, multi-IM, or time-dependent contexts

Multi-hazard physical impact models can be formulated in a vector-valued (e.g., [29]) or a state-dependent format (e.g., [30]). Section 2.4 describes the possible scope of both formats for different hazards. Figure 1a shows examples of vector-valued and state-dependent fragility relationships for dual-hazard interactions. Vector-valued fragility models (surfaces) can be used to model impacts due to concurrent compound hazard intensities (e.g., storm surge and high wind speed in a hurricane; [31]). They are expressed in the form $P(DS \geq ds_i|\mathbf{IM})$, where $\mathbf{IM}$ is a vector of IMs. $P(DS \geq ds_i|\mathbf{IM})$ can be defined using a multi-variate cumulative lognormal distribution function (e.g., [32]), which is a multi-variate generalisation of Eq. 1. A general mathematical formulation for single- or multi-hazard fragility relationships based on various multivariate distributions is provided by Zentner [33], who suggests using the Bayesian information criterion to select the most appropriate one. Note that vector-valued fragility models can also be used to characterise single-hazard conditions (e.g., flood models depending on both water depth and flood duration).

State-dependent fragility models define the fragility of an asset for a given secondary hazard of interest, conditional on its (damage) state after a primary hazard of interest. These models are expressed in the form $P\left(DS(H_k) \geq ds_i|IM(H_k), S(H_j)\right)$ and represent the probability of exceeding the DS threshold (ds_i) for the k-th hazard (H_k), given an IM for hazard k, $IM(H_k)$, and the pre-existing state of the asset after a previous hazard $S(H_j)$, which may refer to damage (e.g., [34]) or an alteration of its structural loading (e.g., [35]), for instance. $P\left(DS(H_k) \geq ds_i|IM(H_k), S(H_j)\right)$ can be determined using Eq. 1, based on data that accounts for $S(H_j)$. State-dependent fragility models for which S coincides with a pre-existing DS implicitly assume that an asset's DS transitions caused by different events are independent, such that the values of DS evolve according to a Markov process, i.e., the present value of DS for the asset only depends on its previous value of DS, rather than its entire history of damage. Note that the state of an asset may also evolve with time, $S(H_j, t)$, and may even be independent of hazard, $S(t)$. $S(t)$ may represent the effect of a physical process (e.g., deterioration due to corrosion) on an asset's ability to resist a hazard loading with a given IM, for instance. Some models [36,37] use a quadratic model for $S(t)$, and consequently for $\theta(S)$ and $\beta(S)$, to capture the corrosion-induced evolution of earthquake fragility for bridge systems for instance.

Multi-hazard, multi-IM, and/or time-dependent vulnerability relationships are usually defined analogously to Eq. 2, adopting similar statistical techniques and assumptions. They can be expressed in a vector-valued (e.g., [38]) or a state-dependent format (e.g., [34]), as appropriate. Multi-hazard and/or time-dependent vulnerability models can be derived directly (such as in [38]) or by combining a set of state-dependent fragility relationships with a damage-to-impact model (such as in [34]). Damage-to-impact models do not require a multi-hazard or time-dependent formulation (i.e., Eq. 4 can still be used) since they directly depend on damage rather than IMs. Multi-hazard and/or time-dependent fragility and vulnerability models can only be adopted if damage is measured consistently across the entire scope of the analysis (Section 2.4 describes the challenges of achieving this).
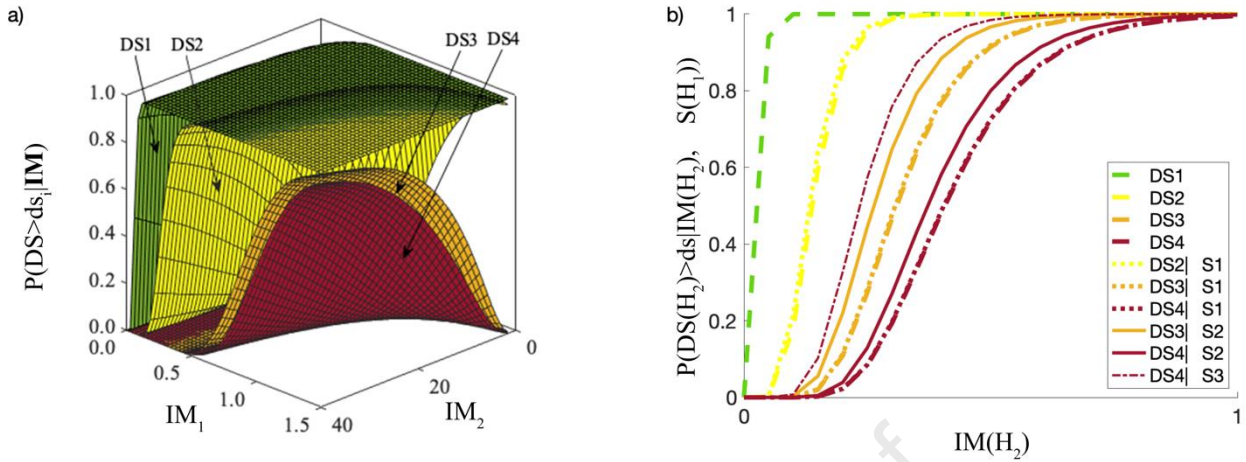
Figure 1: Example a) vector-valued; b) and state-dependent dual-hazard fragility models. IM: intensity measure; DS: damage state; S: state; H: hazard.

2.2. Physical impact models for earthquake-induced ground shaking

5   Earthquakes involve a sudden release of energy from a seismogenic source (e.g., a geological fault). Earthquake-induced ground motions (shaking) represent the surface expression of the resulting propagation of seismic waves (energy) from the source. These motions generate a vibratory response in physical assets. Depending on the dynamic structural characteristics of the asset (e.g., stiffness, strength, ductility capacity, hysteretic behaviour, strength degradation behaviour, plastic mechanism) as well as the nature of the ground shaking experienced at its location, this vibratory response (in the form of

10   displacement/acceleration of its lateral load resisting system) may lead to some level of physical damage in its structural (and non-structural) components. Common damage mechanisms caused by earthquake-induced ground shaking include brittle failure (e.g., in unreinforced masonry and adobe construction), the formation of plastic hinges and shear failures (in reinforced-concrete buildings), anchorage/connection failures (e.g., in timber and steel constructions), and support failures (e.g., in bridges).

15   Typical IMs for earthquake-induced ground-shaking physical impact models typically incorporate some measurement of the amplitude (strength) of the ground motion at the asset's location, such as peak ground acceleration or spectral acceleration at the asset's fundamental period (e.g., [39]). More comprehensive IMs that also account for the spectral shape of the ground-motion record, such as inelastic spectral displacement (e.g., [40]), as well as its duration [41], are becoming increasingly popular because of their superior correlation with the asset's structural response (i.e., their greater efficiency; see Section

20   2.1.1). A more detailed description of the selection of appropriate IMs, as well as a more critical discussion on empirical and synthetic earthquake physical impact models, can be found in Silva et al. [42].

The scientific literature on earthquake physical impact modelling is rich and is likely to be the most extensive across all natural hazards. Discrete DSs considered in asset-level earthquake fragility, and damage-to-impact models represent a progressive deterioration in the asset's performance. A typical set of earthquake-related DSs for a given asset encompasses "minor",

25   "moderate", "extensive", and "complete" categories (e.g., FEMA, Federal Emergency Management Agency [43]). The exact damage implications of each state will depend on pertinent characteristics of the asset in question, such as its type (building, bridge, etc), structural material, geometry and detailing. The most common impact metrics incorporated in seismic vulnerability and damage-to-impact models are economic losses (e.g., [44,45]), casualties (e.g., [46]), and repair/recovery time (e.g., [47]). Recently introduced metrics include debris cover [48] and environmental impact [49].

2.3. Physical impact models for flooding and mass-movement hazards

Floods and mass movements (including debris flows, landslides, lahars, etc.) are gravitationally-driven flows of water and sediment. Both floods and mass movements are triggered by intense rainfall, which is likely to increase in intensity and frequency due to climate change (e.g., [50]). These flows often feature strong morphodynamics that can result in transitional behaviour as erosion and deposition modify the momentum and rheology of the flow (e.g., dilute flash flood transitioning into a more concentrated debris flow as material is entrained).

Fluvial flooding (herein referred to as flooding) occurs when water levels rise in streams, rivers or lakes overflow onto adjacent land. In the vicinity of the built environment, this generally results in low-velocity flows dominated by hydrostatic pressure. Flash floods are short-duration, locally isolated events that feature high peak discharge (i.e., high volumetric flow rates) and are triggered by intense rainfall or by the sudden release of large volumes of water, such as from glacial lake outbursts or dam failure (e.g., [51]). Flash floods often feature much higher flow velocities in the built environment than fluvial floods, where they can entrain loose and eroded debris (e.g., [52]). Because flash floods and debris flows share physical behaviour and potential asset damage mechanisms, and to further differentiate between fluvial and flash floods, flash floods are herein referred to as debris flows, noting that the exact behaviour and damage caused by these flows is a direct function of solids concentration. Landslides are broadly defined to encompass concentrated slips, falls, and flows of debris, rock or sediment down slopes under the influence of gravity. The extensiveness of this definition includes events with characteristic velocities that span at least ten orders of magnitude [53].

Floods and mass movements cause damage to the built environment via four principal mechanisms: 1) pressure in the bulk flow; 2) collisions from debris transported by the flow; 3) erosion scouring foundations; and 4) sediment deposition partially or fully burying structures and other infrastructure (e.g., roads). The pressure in the bulk flow can be split into hydrostatic and hydrodynamic components. The hydrostatic component depends on the flow thickness (h) and bulk density (ρ) of the flow ($\rho g h$, where g is the acceleration of gravity). As the vertical component of most overland flows can be neglected, the hydrostatic pressure component is a reasonable approximation for bulk pressure. However, during strong impacts with buildings and other structures, vertical accelerations in the flow cause the bulk pressure to increase significantly (e.g., [54,55]). The maximum (or peak) pressure on a vertical structure depends on the bulk flow velocity squared (ρv^2, [54,56–58]). Despite their shared physical behaviour and damage mechanisms, physical impacts due to floods, landslides, debris flows, and other mass movements are typically considered separately (excluding some exceptions), and it is challenging to define a unified approach.

The appropriate selection of IMs is crucial to capturing the above mechanisms in related physical impact models. Flood depth is typically employed as an IM for low-velocity flows, such as fluvial flooding [59]. Both flood duration [60] and flood velocity [61] are important to consider as additional IMs in areas with low soil permeability and steep terrain, respectively. The level of contamination in floods (e.g., due to oil) has additionally been incorporated as a secondary IM for flood damage in some models [62,63]. Velocity is used as a single IM for debris flows [64]. Momentum-based IMs, which simultaneously account for a combination of velocity, flow depth, and hydrodynamic stresses, are additionally used to quantify damage (impacts) from debris flows (e.g., [57], [65]). Because debris flows propagate as a wave with a leading front comprised of coarse granular material (e.g., [66,67]), their impacts on structures can be modelled as impulses, such that earthquake-related IMs like spectral displacement can also be leveraged (e.g., [68]). Due to the long timescales involved, defining a single IM for slow-moving landslides is difficult. Physical impact models developed for these hazards have used an IM representing the equivalent cumulative displacement of an area susceptible to landslides [69]. The landslide safety factor [70] has also been used as an IM in slow-moving landslide models since it is related to the mechanical stability of the considered slope. However, there are many challenges in using this measure to quantitatively estimate physical impact, given the large number of parameters required to calculate it and its sensitivity to groundwater infiltration, which is a highly nonlinear and hysteretic physical process.

The physical impact of floods on assets is generally dominated by the contents' loss due to inundation (rather than structural or non-structural damage). As such, most physical impact models for flood-related hazards are empirical vulnerability models and account for economic losses as a function of the flood depth (e.g., [71–73]). These models are generally (and rather confusingly) referred to as "depth-damage" vulnerability functions under the implicit assumption that monetary expenses are

6

a reasonable proxy for physical damage. Synthetic models such as INSYDE (IN-depth SYnthetic model for flood Damage Estimation, [74]) present component-by-component vulnerability functions in terms of monetary losses. Other types of flood impacts captured in developed models include casualties [75] and repair time [76]. Fragility functions are becoming increasingly available for flooding hazards (see [77] for a review), the most recent being those in [71], which describe a series
5   of component-by-component DSs that directly correspond to probabilistic economic loss outcomes for pluvial and fluvial flooding events. However, damage-to-impact models for flooding are rare and may not be hazard-specific [76]. In addition, the development of physical impact models for both debris flows and landslides is limited compared to flooding and earthquake hazards. This can be attributed to the complex dynamics of debris flow and landslide hazards [78], difficulties in estimating the associated dynamic responses of structures [54], and a lack of significant potential to cause human losses (in the case of
10   slow-moving landslides). Exceptions include: (1) fragility models for debris flows that describe DSs using terminology adopted from earthquake fragility models (see Section 2.2 and [68,79,80]); and (2) fragility and vulnerability curves for landslides [69] that use similar DSs to those described for earthquakes (see Section 2.2) and represent impact in terms of a continuous equivalent damage level.

2.4. Physical impact models for multi-hazard and time-dependent contexts

15   Many regions in the world are prone to more than one natural hazard, such that structures/infrastructure systems can be subjected to more than one hazard during their lifetime (e.g., [81]). Effective risk-informed decision-making and/or risk management prioritisation is only possible if all relevant threats are considered and analysed (e.g., [82–86]). This requirement is compounded by the fact that two or more hazards affecting the same location in a relatively short period could result in physical or social impacts greater than the sum of the effects from each individual hazard [87,88]. A multi-risk approach,
20   accounting for the interaction of risks from multiple hazards, is therefore necessary. This type of approach should incorporate interactions at the level of hazard, exposure, and physical/social impact ([90]; therefore, multi-hazard fragility/vulnerability models play a significant role. In addition, a lifecycle risk analysis is likely needed to accurately consider the interaction of single or multiple hazard events of different occurrences and resulting intensities. This involves simulating the time between different events and may require time-dependent (or state-dependent) physical impact models.
25   Gill and Malamud [86] define multi-hazard interactions to include situations in which: a hazard triggers one or more other hazards; the probability of a hazard is increased or decreased; there is a spatiotemporal coincidence of different hazards. As pointed out by [89], these classifications share characteristics with further studies that identify the following three mechanisms of interaction: the trigger or causality, usually referred to "domino effects" or "triggered hazards"; the influence, indicating increased/decreased probability or magnitude, without acting as a trigger; the independent coincidence, when the spatial or
30   temporal scale of independent hazards partially intersects. However, the classification proposed by Zaghi et al. [90] which also considers other risk components apart from hazard, fits best with the scope of this study. This classification considers two levels of interaction: 1) level-one interactions that occur through the source, time and/or frequency of occurrence of two or more hazards and are independent of the presence of physical assets (e.g., earthquake-tsunami sequence); 2) level-two interactions, which occur through the effects of the hazards on the site of interest, accounting for the presence of physical
35   assets, and capture system-level disruptions as well as social and economic effects (e.g., flood-induced scour may increase a bridge's earthquake fragility, although the earthquake IM is not affected by the scour). Bruneau et al. [91] note that the classification in Gill and Malamud is independent of the effects of the hazards, and it, therefore, only applies to level-one interactions. This Section only deals with physical impact modelling related to level-two interactions (i.e., that involve a modification of a fragility/vulnerability curve due to cumulative damage to an asset) since level-one interactions do not require
40   changes to the underlying impact models. Thus, repeated instances of the same hazard (e.g., earthquake sequences, compound flooding) are considered multiple hazards.

Physical impact models that adequately capture level-two interactions must be based on a consistent definition of structural and non-structural damage. These models should adequately capture the damage mechanisms relevant to the considered hazards, also including their cumulative effects (i.e., how damage due to one hazard may reduce safety margins for the
45   considered asset/component, thus increasing damage from other hazards). Most multi-hazard physical impact models are based on uncoupled damage scales for each hazard (e.g., HAZUS, [43])., but some attempts to incorporate consistent damage scales have been made in the literature (e.g., [92,93]). Describing cumulative damage requires defining an ad-hoc scale that depends on the specific asset and hazards, (e.g., [94]). Synthetic, physics-based models of an asset that capture damage accumulation

under different hazards are possibly the only viable approach to address the above-mentioned challenges. (In fact, it is unlikely that empirical damage data for specific asset/hazard combinations are available.) Furthermore, these synthetic models must use appropriate static or dynamic mechanical characterisations of the asset materials and components to capture the interactions of the relevant damage mechanisms. For example, to model the interacting effects of wind and earthquake on a building, it is

5   necessary to characterise the material hysteresis (i.e., the evolution of their stiffness under unloading-reloading cycles) and its strength degradation under sustained cyclic deformation (e.g., [95]).

Quantitative multi-hazard physical impact models are comparatively less common in the literature than single-hazard ones. Rather than providing a thorough literature review, which is outside the scope of this paper, this section selects examples of multi-hazard physical impact models for buildings and bridges to qualitatively assess model availability in terms of the number

10   of considered hazards and their nature (e.g., synthetic, empirical). Most available models involve fragility relationships for two hazards, with some exceptions discussed below. Figure 2 summarises dual combinations of hazards for which it was possible to find at least one quantitative physical impact model.

Most multi-hazard physical impact models for buildings focus on sequential earthquake events/ground motions (e.g., [30,96–99]) and take the form of state-dependent fragility models for different types of buildings and DSs of interest. Some such

15   fragility models include time-dependent considerations (measured using a consistent damage scale), such as the effect of structural ageing on concrete buildings during earthquake sequences (e.g., [100]). Petrone et al. [101], among others, provide state-dependent fragility models for reinforced concrete buildings exposed to earthquake-tsunami sequences. Earthquake-landslide state-dependent fragility models are provided in [102], for example. Fragility models combining earthquake and wind actions are available in [103] and [104], for instance. The model in [35] describes the state-dependent earthquake fragility of

20   buildings that are pre-loaded with snow. The proposed model in [105] relates to the blast fragility of reinforced concrete structures in the presence of seismic risk. Compound flooding, related to the concurrence of multiple hazard drivers (e.g., heavy rainfall, extreme river flow, and storm surge), can be effectively modelled using standard depth-damage flood vulnerability models based on the maximum-in-time water depth as an IM (e.g., [31]). Realistic modelling of hurricane impact requires a multi-hazard approach involving wind-induced pressure, surge and waves. The physical impact model in [106]

25   accounts for the probability of structural damage by combining vector-valued flood fragility models, vector-valued surge-wave fragility models, and wind pressure fragility functions. Luo et al. [107] propose a framework to produce physics-based models for sequentially- and concurrently-occurring debris flow impacts. Models in [108] account for fragility due to earthquakes and pyroclastic flows that follow ash fall events.

Examples of multi-hazard vulnerability modelling involve the flood-induced scour on bridge foundations (e.g., [109]), the

30   combined effect of flood-induced scour and ground shaking (e.g., [110,111]), ground shaking and liquefaction on bridges (e.g., [112]), liquefaction and lateral ground displacement (e.g., [113]), earthquake sequences (e.g., [114]), and earthquake-tsunami sequences (e.g., [115]). A more-detailed literature review on multi-hazard infrastructure vulnerability models (including roads, bridges, embankments, tunnels, retaining walls, slopes, etc.) is provided in [116], which includes liquefaction, landslides, debris flow and flood and the combined effects of flood-induced scouring and earthquakes. According to this review, most

35   multi-hazard vulnerability models have been developed for bridges.

|	Earthquake	Landslide	Liquefaction	Tsunami	Flood	Strong wind	Snow load	Debris flow	Ash Fall	Pyroclastic flow	Scour	Lateral spreading	Blast
Earthquake	X												
Landslide	X	X											
Liquefaction	X												
Tsunami	X												
Flood					X								
Strong wind	X				X								
Snow load	X												
Debris flow								X					
Ash Fall	X												
Pyroclastic flow										X			
Scour	X				X								
Lateral spreading		X											
Blast	X												

Figure 2 Availability of quantitative multi (dual)-hazard physical impact models. Each mark indicates that the literature includes at least one (building or bridge) physical impact model for the considered dual-hazard combination.

5 The choice of physical impact models for a given analysis must consider whether the adopted risk model can account for lifecycle considerations. A lifecycle risk analysis should account for the probabilistic distributions of the hazard-event occurrences, use an appropriate multi-hazard model to quantify relevant impact metrics, record the state of the asset after each event, and finally combine the results to calculate the probability distribution of the lifecycle impact (e.g., [117]). Choosing an appropriate physical impact model in this context depends on the types of successive events and their inter-event time; the

10 repair (or recovery) strategy in place for the asset (which affects the probability of incomplete repair for a given DS and time); and the considered time horizon for the analysis.

Lifecycle risk analysis models considering only one hazard type (note that multiple events of the same hazard type are regarded as multiple hazards, as discussed above) in the literature often consider an "instantaneous" repair of the considered asset after each event (e.g., [118]). These models require a single-hazard physical impact model, which should be time-dependent to

15 capture any asset degradation between two events; in this case, $S = S(t)$ from Section 2.1.1. Lifecycle models considering triggered hazards (e.g., [119] for mainshock-aftershock earthquake sequences) require an $S = S(H_j)$ state-dependent physical impact definition. Multi-hazard (dependent or independent) lifecycle risk models that consider the probability of repairs being completed before the next event (e.g., [120] for earthquakes and flood-induced scour) require appropriate $S = S(H_j, t)$ state-dependent physical impact models. Lifecycle risk models that relax the Markovian assumption on the DS of the asset require

20 n-variate vector-value physical impact models (as defined in Section 2.1.1), where n is the potential number of hazard events (of the same or different type) that could occur before the asset is repaired. Choosing n, and the considered hazard types, may be determined based on the considered repair strategy for the asset. However, to the best of the authors' knowledge, no quantitative method is currently available to accomplish this goal.

3. Proposed characterisation procedure for physical impact models

25 The proposed methodology (Figure 3) for scoring, selecting, and developing physical impact models starts after selecting one or more natural hazards, independent or interacting, which are relevant for a selected case-study area. Although this is not strictly part of the proposed methodology, a useful tool to assist this choice is Thinkhazard (https://thinkhazard.org, last accessed June 2022), which provides a general view of hazard susceptibility on a global scale. Next, assets within the considered area are grouped into classes according to a taxonomy model, which may require different sets of general

parameters specific to the identified asset class and hazards (e.g., occupancy, geometry parameters, design level). Section 3.1 discusses codifying the required asset class characteristics in a multi-hazard taxonomy string and the minimum set of these parameters required for different hazard/asset-class combinations. The taxonomy string is then used to map the hazard/asset-class combination to relevant candidate impact models. As discussed in Section 3.2, this process can involve models from
5   interactive databases, model compendia, or literature reviews. It should incorporate general considerations of the trade-off between simplicity, accuracy, and data requirements of the overarching risk model. The considered candidate models are then ranked according to a set of criteria to determine the most appropriate one (Section 3.3). If the above search does not provide any satisfactory result, the proposed procedure involves developing new physical impact models based on an empirical or synthetic (analytical or numerical) approach, as detailed in Section 3.4. The proposed procedure should be applied for multiple
10   asset classes in parallel to determine whether physical impact models for different classes can be derived using a consistent methodology, which would lead to a desirable consistency in the damage/impact estimations of the considered risk assessment. The main goal of this procedure is to facilitate the consistent appraisal and selection of a set of candidate physical impact models for use within risk modelling applications. The procedure may also be beneficial for application to new physical assets to be constructed as part of a risk-informed urban development process. Any values provided for relevant input parameters
15   (e.g., specific criteria, threshold values for screening, scoring schemes, and weights; see Section 3.2 for more details) are only provided as recommendations; users are encouraged to adjust these parameters according to their specific needs. A code repository supporting the application of this procedure is provided at <u>github.com/robgen/rankFragilityVulnerability</u> (last accessed June 2022).
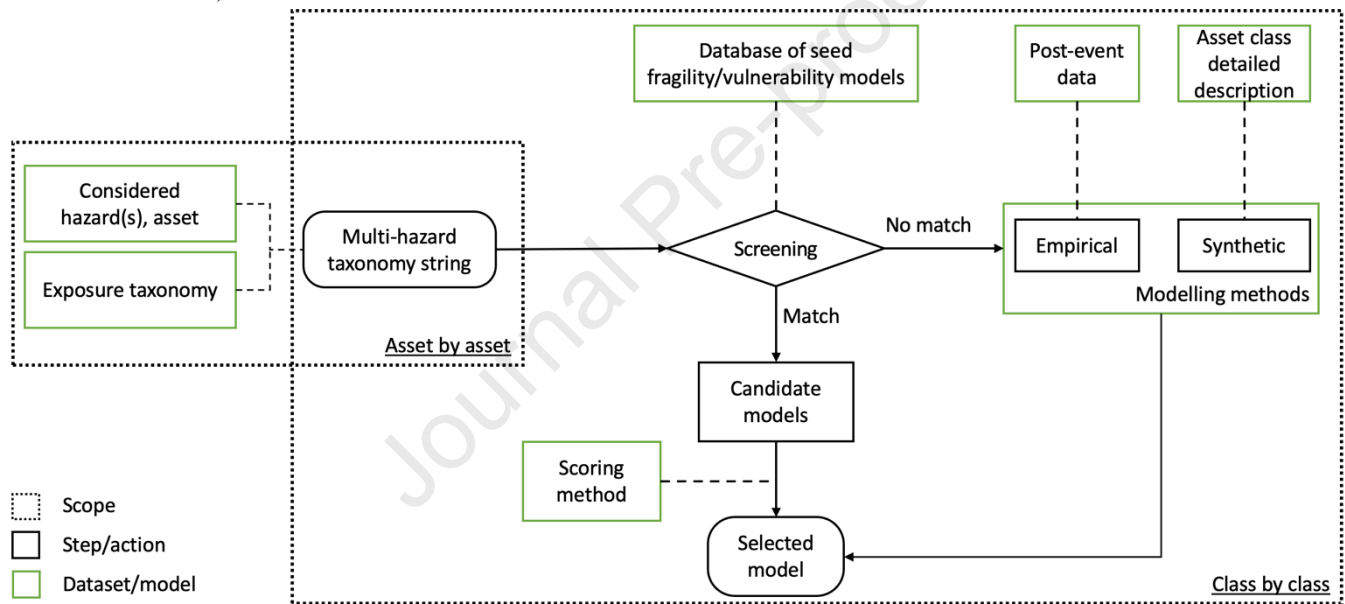
20   **Figure 3 Proposed methodology to score and select physical impact models for a given asset class**

3.1. Preliminary phase: defining the exposure taxonomy string of the asset classes

The proposed procedure starts with identifying the physical attributes of the asset classes directly correlated with the physical impacts induced by relevant natural hazards. For example, the lateral load resisting system attribute is used to determine earthquake and wind fragility (among other hazards), the presence of a basement is relevant to flood fragility, and the roof
25   typology (and its features) is a factor that influences hurricane fragility. The building occupancy type affects, for instance, the likely distribution of building occupants during any given day. For example, a school will be (near) fully occupied during certain hours on school days, predominantly by children. Moreover, the occupancy type defines the components likely to be present within a building. For example, industrial buildings contain machinery. These attributes are used to develop a series of exposure taxonomy strings, which consist of a combination of alphanumeric labels that contain asset-class-specific attribute

information. These strings are an ideal data format for storage within a database (e.g., Geographic Information Systems, GIS) to facilitate interaction between the exposure and vulnerability modules of a risk model.

A taxonomy string should be general enough to account for multiple hazards, scales, and asset classes. The global exposure database for all (GED4ALL [121]) best meets the above criteria since it facilitates links to many existing databases of physical
5 impact models and is therefore leveraged in the proposed methodology. It covers buildings, roads, railways, bridges, pipelines, storage tanks, power grids, energy generation facilities, crops, livestock, forestry, and socio-economic data. This taxonomy was developed considering earthquakes, volcanoes, floods, tsunamis, storms, cyclones and drought. GED4ALL, also referred to as global earthquake model (GEM) taxonomy 3.0, is the multi-hazard generalisation of the GEM 2.0 taxonomy [122], which is in turn derived from t previous taxonomies such as those of ATC-13 [123], the European macro-seismic scale (EMS-98,
10 [124]), HAZUS [125], and PAGER-STR [126].

The GED4ALL taxonomy strings include different attributes for different asset types and facilitate three different levels of refinement/detail (from Level 1 to Level 3) in the input that accommodate various degrees of available data. This flexibility could be particularly convenient for data-scarce regions which are especially prevalent in developing countries. Table 1 and Table 2 respectively provide the GED4ALL attributes for buildings and bridges, suggesting those that are strictly required
15 versus optional in relation to the physical impact modelling of different hazards. An example of a Level 1 string is CR/H:2/LWAL/RES, which indicates a two-storey reinforced concrete residential building with a wall lateral load-resisting system. Level 2 information could include data on the material technology, for instance, which may be cast in place (CR+CIP) in the above example. A Level 3 string could include secondary information related to primary (Level 2) structural irregularities, such as the presence of torsion eccentricity and a re-entrant corner for the above example
20 (IRIR+IRPP:TOR+IRPS:REC). Extensive documentation for each asset class is provided at docs.riskdatalibrary.org/ged4all.html (last accessed June 2022). In addition, this webpage indicates that an automatic tool to convert a set of attributes into a single taxonomy string, similar to "TaxtWeb" (platform.openquake.org/taxtweb, related to the GEM2.0 taxonomy, last accessed June 2022), is under preparation.

The GED4ALL attributes are mapped to the keys (or tags) in the OpenStreetMap database, a large open-source mapping
25 repository (openstreetmap.org). Thus, it is possible to derive GED4ALL taxonomy strings for exposure data using the export tool developed by the Humanitarian OpenStreetMap Team (export.hotosm.org, last accessed June 2022). Finally, the GED4ALL repository (github.com/gem/ged4all, last accessed June 2022) includes software for converting taxonomy strings to the natural hazard risk markup language (NRML), enabling compatibility with other exposure taxonomies/models. This can be done using the input preparation tool by GEM (platform.openquake.org/ipt, last accessed June 2022).
30

Table 1 GED4ALL attributes for buildings exposed to different hazards. OSM: OpenSteetMap; R: required; O: optional; EQ: earthquake; FL: flood; DF: debris flow; TS: tsunami; LA: landslide; FI: Fire; WI: wind; VA: volcanic ash.

Attribute	OSM Key	EQ	FL	DF	TS	LA	FI	WI	VA
Direction	building:direction	O	O	O	O	O	-	O	-
Material of LLRS	building:lateral:material	R	R	R	R	R	O	R	R
Lateral Load Resisting System (LLRS)	building:lateral:system	R	R	R	R	R	O	R	R
Height	building:levels	R	R	R	R	R	R	R	R
Date of construction or retrofit	building:age	R	O	O	R	R	O	R	R
Surroundings	building:adjacency	O	O	O	O	-	O	-	-
Occupancy	building	R	R	R	R	R	R	R	R
Shape of building plan	building:shape	O	O	O	O	O	R	R	-
Structural irregularity	building:irregularity	O	O	O	O	O	-	-	O
Ground floor hydrodynamics	ground_floor	-	-	O	O	-	-	-	-
Exterior walls	building:material	O	O	O	O	-	O	O	-
Roof shape	roof:shape	-	-	-	-	-	O	R	R
Floor system material	floor:material	O	O	O	O	O	O	O	O
Foundation	building:foundation	O	O	O	O	O	-	O	-
Fire protection	building:fireproof	-	-	-	-	-	R	-	-

35 **Table 2 GED4ALL attributes for bridges exposed to different hazards. Notation as per Table 1.**

11

Attribute	OSM key								
General material	bridge:material	R	R	R	R	R	R	R	R
Super structure	bridge:structure	R	R	R	R	R	R	R	R
Deck characteristics	bridge:width;length;height	R	R	R	R	R	R	R	R
Deck structural system	bridge:support	O	O	O	O	O	O	O	O
Pier to deck connection	pier:connection	R	O	O	R	R	O	R	R
Pier to superstructure connection	pier:superstructure	O	O	O	O	O	O	O	O
Number of piers	bridge:total_piers	R	R	R	R	R	R	R	R
Shape of pier section	pier:shape	O	O	O	O	O	-	R	-
Pier height	pier:height	O	O	O	O	O	-	-	O
Spans	pier:span	R	R	R	R	R	R	R	R
Connections to the abutments	Abutment:connection	R	R	R	R	R	O	R	O
Bridge configuration	bridge:configuration	O	O	O	O	O	O	O	O
Level of seismicity	bridge:seismicity	O	-	-	-	-	-	-	-

3.2. Screening phase: selecting candidate physical impact models

This step of the procedure involves identifying a list of candidate physical impact models among a given set of seed options. The ideal resource for performing this task would be an extensive database of single-hazard and interacting multi-hazard physical impact models that account for multiple asset typologies consistent with the GED4ALL taxonomy. This type of
5 database should include a search engine actioned by the GED4ALL taxonomy string and should be constantly and systematically updated with relevant advancements in the literature. Although this type of resource is not yet available, related research efforts are ongoing, particularly around storing relevant attributes (e.g., analytical vs numerical vs empirical) of physical impact models (e.g., [127] for earthquake fragility and vulnerability, [128] for flood vulnerability), or producing harmonised data schemas that improve data interoperability within the different modules of a risk model (e.g., [129]).
10 This screening phase of the procedure involves:

1) Defining three fundamental parameters: asset location, asset taxonomy string, and considered hazards. To maximise the model search results, these parameters should be defined with different levels of refinement. For example, "location" may be defined as "Kathmandu", "Nepal", or "Asia"; "taxonomy string" may be defined using only level-one GED4ALL attributes, or level-one and -two attributes combined, or also level-three attributes; "hazards" may be
15 considered singularly, in relevant pairs or in relevant triplets, etc.;

2) Performing an automatic search in any available interactive database of physical impact models (with examples discussed below; and the ideal version of this database described above). This should be performed multiple times for any combination of refinement in the above three parameters, starting from their most-refined definitions. Each match encountered during these searches constitutes a candidate model;

20 3) Performing a manual search in any non-interactive available model compendium, literature review study, and regional/global models (with examples discussed below), as per point 1. Any match should be added to the candidate model list;

4) Performing a specific literature review for the most-refined definition of the three fundamental parameters that also accounts for specific user requirements (e.g., time-dependent models accounting for material ageing, specific IMs).
25 This step maximises the specificity of the matching models, whereas steps (2) and (3) maximise the number of matches;

5) Screen the candidate models to determine a subset to be ranked for quality in the subsequent phase. When screening, users should consider the possibility of developing ad-hoc adjustments to improve any given model. An example is to provide a modification coefficient to allow a physical impact model to consider an extra exposure parameter as an
30 input (e.g., a height-dependent modifier to a model not accounting for building height, Section 4.4). The screening process is carried out according to three criteria: appropriateness of the damage scale (for fragility models) or the impact metric (for vulnerability and damage-to-impact models) concerning the considered application; the amount of extrapolation required to adopt a given model for the considered application; and the available documentation for a given model. The last criterion directly relates to the model scoring phase in the next step of the proposed procedure,
35 which should avoid excessive guessing. Table 3 provides a set of example qualitative acceptance (i.e., screening) thresholds for the three criteria above, which can be modified appropriately according to user judgement for a considered application.

Table 3 Model screening criteria: minimum thresholds for acceptance [N_{ds}, R_{im}, N_{hp} are defined by the user; example values: N_{ds}=1, R_{im}=20, N_{hp}=80]

Screening criterion	Suggested acceptance threshold
Damage/impact appropriateness	Required DSs are defined (or N_{ds} DSs are missing). Required impact metric is modelled.
Required extrapolation	Required IM range is covered (or R_{im}% extrapolation needed)
Documentation	Documentation justifies N_{hp}% of the model's assumptions (e.g., damage scale, IM selection, fitting methods)

3.2.1. Available interactive databases of candidate models

5 GEM provides an online tool (platform.openquake.org/vulnerability/list, last accessed June 2022) for mapping a GEM2.0 building taxonomy string to different candidate empirical or synthetic physical impact (or structural capacity curve) models for earthquakes [130]. Each model in the database is associated with a scientific publication and is classified according to geographical applicability, model typology (synthetic or empirical), adopted IM, etc. The tool also allows users to add more models to the database. A similar tool (vulncurves.eu-risk.eucentre.it, last accessed June 2022) related to physical earthquake

10 vulnerability modelling (empirical or synthetic) of the European Seismic Risk Model, (ESRM20 [131] matches GEM3.1 building taxonomy strings to relevant physical impact models (and capacity curves) for European building classes. Stefanoiu et al. [132] provide an online database (thebridgedatabase.com/existing-fragility-curves/, last accessed June 2022) of earthquake fragility relationships (mainly synthetic) for bridges that can be augmented with user input. Each bridge class is defined using an ad-hoc taxonomy. Each model is classified according to the model type (synthetic or empirical), adopted IM,

15 DS thresholds, etc., and is associated with a scientific publication.

Alam et al. [133] introduce the Cascadia lifelines program (CLiP) fragility function online database (clip.engr.oregonstate.edu, last accessed June 2022), which involves earthquake and tornado fragility relationships (empirical and synthetic) for a large set of lifeline assets within electric, water, wastewater, and transportation systems. Each model is classified similarly to that for the abovementioned databases, although CLiP adopts ad-hoc taxonomy strings. The fragility function manager [134] of

20 the SYNER-G project (Systemic Seismic Vulnerability and Risk Analysis for Buildings, Lifeline Networks and Infrastructures Safety Gain, [135]) is an MS Windows-based application for storing, visualising and managing earthquake fragility relationships (both empirical and synthetic). The database classifies assets based on the SYNER-G taxonomy (largely consistent with that of GED4ALL). It includes models for buildings, bridges, road infrastructure, oil and gas systems, and lifelines, including electric, water, and wastewater. To the best of the authors' knowledge, this is the only interactive database

25 that includes time-dependent models for the corrosion-related ageing of bridges. The vulnerability module of the CAPRA (Central American Probabilistic Risk Assessment platform, [136]) software is an MS Windows-based application to create, visualize and compare new and existing multi-hazard vulnerability functions, expressed in terms of economic or human loss. The software uses a simple analytical methodology to obtain new vulnerability functions based on a few parameters. The software involves vulnerability functions for multiple hazards and assets classified according to an ad-hoc exposure taxonomy

30 model.

The flood damage model repository ([137], github.com/mattrighetti/fdm-repository-backend, last accessed June 2022) provides a collection of 42 empirical flood physical impact models related to residential, commercial and industrial buildings, agricultural land, and transport infrastructure. Although the asset classes in the database are not associated with any specific exposure taxonomy strings, the considered models are classified according to different parameters, including their geographical

35 applicability, flood type, model type (e.g., synthetic or empirical), and the adopted IM. The tool by RiskChanges (riskchanges.org/app//#/datamanagement/vulnerability, last accessed June 2022) comprises empirical and synthetic vulnerability relationships for multiple hazards and different asset types. This open database incorporates different single-hazard models (e.g., wind, drought, fire, technological, earthquake, volcano), allowing users to input new models. To the best of the authors' knowledge, this is the only interactive tool collecting models for different asset typologies and different hazards.

40 This database adopts an ad-hoc exposure taxonomy string and only includes a small number of models. Moreover, this database does not include multi-hazard fragility/vulnerability models.

3.2.2. Available non-interactive databases and model compendia

A short, non-exhaustive collection of physical impact model compendia and global models is herein provided. Rossetto et al. [138,139] provide a compendium of empirical earthquake fragility and vulnerability relationships for different building classes worldwide (last updated April 2014; available at ucl.ac.uk/epicentre/resources/gem-vulnerability-databases, last accessed June 2022). Calvi et al. [139] provides a review of nearly 100 synthetic and empirical earthquake fragility/vulnerability models developed over three decades. The European tsunami risk service provides a compendium of synthetic and empirical fragility curves for buildings subjected to tsunamis (github.com/eurotsunamirisk/etris_data_and_data_products, last accessed June 2022).

Regional- or global-level models provide consistent results across different asset classes, which is particularly desirable within risk models and could be considered within the proposed procedure. Moreover, these models will likely produce matches within the proposed screeing procedure. A non-exhaustive list of these models is provided herein. [140] provide an analytical earthquake fragility and vulnerability model covering the most common building classes at a global scale. Among many others, some studies provide physical earthquake impact models for asset classes in Iran [141], northeast India [142], Peru [143], China [144], and Pakistan [145]. The Joint Research Centre (JRC) of the European Commission produced a comprehensive global model of empirical flood depth-damage vulnerability functions for a variety of assets [146]. The functions are available in a tabular dataset at publications.jrc.ec.europa.eu/repository/handle/JRC105688. The JRC functions were developed empirically using data from different continents (i.e., Europe, Asia, Africa) and considered residential, commercial and industrial occupancies. These functions can be readily adapted to provide local and regional loss estimations (e.g., [147]). The HAZUS depth-damage regional vulnerability functions are accessible in an online package (CRAN.R-project.org/package=hazus, last accessed June 2022).

3.3. Scoring phase: selection of the most suitable model

For a given asset class, selecting the most suitable candidate model is ultimately a subjective decision of the user. Nonetheless, the selection process can be supported by a rational-yet-qualitative model scoring system based on key attributes related to the suitability of a given model.

This step of the proposed procedure enhances and combines different existing model scoring methods for single-hazard conditions and/or a single model typology. These methods provide criteria to evaluate the quality of asset-level physical impact models and are mainly focused on earthquakes. Porter [148] proposes a scoring system for analytical or empirical earthquake fragility models based on five criteria (data quality, relevance, rationality, documentation, and overall quality) and four scoring levels (superior, average, marginal, or not applicable). Meslem et al. [149] refined the previous scoring system for analytical earthquake fragility models. Rossetto et al. [150] further generalised the approach by Meslem et al. for analytical and empirical earthquake fragility and vulnerability models. The resulting scoring system is based on ten criteria grouped into four categories: data quality, representativeness of a specific class, rationality (e.g., obeying first principles), and documentation quality. Finally, Alam et al. [133] provide a two-step scoring system for earthquake and tornado fragility models of lifeline infrastructure. Based on a set of 16 criteria (related to regional applicability, IM, structural class, damage characterisation, data quality, analysis model and method, fragility derivation), the system involves 1) eliciting a group of experts to score each criterion in terms of importance; and 2) aggregating the expert's responses to assign scores to each criterion.

Leveraging the above literature, this study proposes a scoring system for multi-hazard physical impact models related to different asset types and analysis methods. The adopted criteria are based on those in Rossetto et al. [150] but incorporate the following enhancements: (1) generalisation for a multi-hazard scope; (2) removal of criteria already considered in the screening phase (e.g., documentation); (3) addition of some bespoke criteria (details to follow); and (4) grouping of criteria to facilitate the final scoring part of the proposed procedure. Given a set of candidate physical impact models, the scoring phase of the proposed procedure involves:

1) Scoring each candidate model against four suggested criteria: relevance, statistical refinement, model quality (defined differently for empirical or synthetic models), and user-defined requirements. Each criterion involves one or more attributes, which should be qualitatively scored "high", "medium", or "low" according to the scheme described in Table 4. The "relevance" criterion involves the "geographical area" attribute, which captures the representativeness of a given model for a given area, "asset characteristics", which considers how the parameters of the asset's structural

14

details, materials, and geometry within the model reflect those required for the considered asset class, and "IM", which is related to the sufficiency and efficiency of the adopted IM(s). The "statistical refinement" criterion involves the "uncertainties" attribute, related to the refinement of the treatment of uncertainty for a given model, and "first principles", which accounts for any functional inconsistency in the model (e.g., crossing of fragility functions for different DSs; unreasonably large/small maximum value of the impact metric of a vulnerability function). For empirical models, the "model quality" criterion includes the attributes "impact observations" and "IM observations" that are related to the level of error/bias involved in the fitted data, "constrained asset class" that captures how well the fitted data is suited to a single asset class, and "data quantity", which involves the number of IM vs damage/impact observations used to fit the model. For synthetic models, this criterion involves "fidelity to mechanics", which captures how well an analytical/numerical model reflects the mechanics of an asset subjected to one or multiple hazards, and "aggregation level", which reflects the level of sophistication involved in the model (e.g., asset- vs component-level models). The attribute (and criterion) "user-defined requirements" reflects the level of compliance of the selected model with a set of user-defined features (e.g., time/state dependency, consistency of model assumptions across different asset classes). Note that although the model typology (e.g., synthetic vs empirical) can generally be considered a user-specific requirement, it can also be indirectly related to other requirements (e.g., no time-dependent empirical models are available, and therefore a synthetic model must be selected). Any attribute related to IMs should be disregarded when scoring damage-to-impact models. This set of criteria and attributes are suggested based on the available literature information and engineering judgement of the authors. Consistent with the spirit of this selection procedure, users are encouraged to add or remove specific criteria/attributes according to their specific needs;

2) Each criterion has a prescribed weight. The analytic hierarchy process (AHP; [151]) is used to produce a mathematically consistent definition of the weights, which has already been successfully applied to engineering decision-making problems (e.g., [152]). According to this procedure, the user expresses an opinion on every possible pairwise comparison among the criteria. Each opinion quantifies how much criterion j is more/less important than criterion k. The results of the comparisons constitute a decision matrix. The desired weights are proportional to the first eigenvalue of this matrix. Further details can be found in [151]. The suggested weights for the criteria are 25% for "relevance", 15% for "statistical refinement", 40% for "model quality", and 20% for "user requirements". However, users are encouraged to apply AHP for their specific circumstances to derive case-specific weights;

3) Given the adopted weights, scoring of the available models is carried out according to the technique for order preference by similarity to an ideal solution, or TOPSIS [153]. This procedure has been deemed suitable for engineering decision-making problems (e.g., [154]). First, the user scores each candidate model against the four criteria (using the qualitative scores "low, medium, or high"). The score assigned to a given criterion is the minimum score obtained for all of its attributes (e.g., the minimum score among the attributes "fidelity to mechanics", and "aggregation level" quantify the score of the "model quality" criterion for synthetic models. For example, this approach penalises a refined component-by-component numerical model that neglects relevant damage mechanisms and/or impact sources). To be used as an input of TOPSIS, these qualitative scores should be expressed as numerical values. Alternatively, triangular fuzzy numbers may be used in a qualitative TOPSIS approach [155]. It is herein suggested to use 1, 2, and 3, respectively, for low, medium, and high. However, users are encouraged to test the sensitivity of the final result to these values and alter them if required. The weighted scores for a given criterion are used to define the ideal best and worst models, and the most suitable model maximises a trade-off between the distances from the ideal worst and best models [151].

Table 4 Model scoring system: definition of scores for each attribute. [ATT, OBS_1, OBS_2, OBS_3, $bins_1$, $bins_2$, obs_1 are defined by the user; example values: ATT=4, OBS_1=20, OBS_2=200, OBS_3=20, $bins_1$=5, $bins_2$=10, obs_1=20]

Criterion: Attribute	Score	Description
Relevance:	High	Model defined for the required city (e.g., Kathmandu)
Geographical area	Med	Model defined for the required country (e.g., Nepal)
	Low	Model defined for the required region (e.g., South Asia)

15

	High	Model matching structural detailing, geometry, and materials parameters appropriate for the asset class
Relevance: Asset characteristics	Med	Geometry and materials parameters appropriate for the asset class, structural details inappropriate or unavailable
	Low	Materials params. appropriate for the asset class, geometry and structural details inappropriate or unavailable
Relevance: IM	High	Adopted IM(s) clearly sufficient/efficient for the required application
	Med	-
	Low	Adopted IM(s) clearly not sufficient/efficient for the required application
Statistical refinement: Uncertainties	High	Appropriate assumptions. Goodness of fit demonstrated. Aleatory (and possibly epistemic) unc. considered
	Med	Appropriate assumptions. Inappropriate aleatory unc. considered
	Low	Inappropriate assumptions (e.g., unsound statistical distributions)
Statistical refinement: First principles	High	Physically sound models (e.g., fragility curves for different DSs not crossing; reasonable maximum)
	Med	Minor first-principle issues (e.g., fragility curves for different DSs cross outside required IM range)
	Low	Relationships not physically sound (e.g., fragility curves for different DSs cross)
Model quality (empirical): Impact observations	High	Damage scales/impact measures clearly defined. Negligible non-sampling errors (see Section 3.4)
	Med	Damage scales/impact measures clearly defined. Non-sampling errors treated with unchecked assumptions.
	Low	Damage scales/impact measures ambiguously defined (e.g., two assessors may assign different DSs for the same situation). Non-sampling errors not reduced
Model quality (empirical): IM observations	High	IM data directly measured or estimated accurately. IM data predicted-vs-true error investigated
	Med	-
	Low	IM data directly measured or estimated inaccurately. IM data predicted-vs-true error not investigated
Model quality (empirical): Constrained asset class	High	Empirical dataset filtered using asset class definition according to GED4ALL, or with similar attributes
	Med	Asset class defined as per "High", but some aggregated attributes (e.g., different heights considered together)
	Low	Asset class defined with less than ATT attributes
Model quality (empirical): Data quantity	High	Continuous functions: more than OBS_2 observations; min $bins_2$ IM bins; min obs_2 observations per IM bin. Discrete functions: more than OBS_2 observations; min obs_2 observations per IM bin
	Med	Continuous functions: between OBS_1 and OBS_2 observations; between $bins_1$ and $bins_2$ IM bins; min obs_2 observations per IM bin. Discrete functions: min obs_1 observations per IM bin
	Low	Continuous functions: less than OBS_1 observations; less than $bins_1$ IM bins. Discrete functions: less than OBS_3 observations
Model quality (synthetic): Fidelity to mechanics	High	State-of-the-art. All relevant damage mechanisms/impact sources considered. Sound parameter characterisation
	Med	Minor simplifications of relevant mechanics (e.g., less-relevant damage mechanisms/impact sources neglected). Sound parameter characterisation
	Low	Major simplifications of relevant mechanics (e.g., fundamental damage mechanisms/impact sources neglected). Unsound parameter characterisation (e.g., excessive strength assumed for a key structural member)
Model quality (synthetic): Aggregation level	High	Calibrated using component-by-component analysis. Each component modelled explicitly
	Med	Calibrated using subcomponent analysis (e.g., aggregating components at the same building storey)
	Low	Asset-level model. Aggregating all sources of damage or impact
User-specific requirements	High	Model exactly reflects all the user requirements
	Med	Model not complying with minor user requirements (e.g., required time dependency not covered)
	Low	Model not complying with major user requirements (e.g., required state dependency not covered)

3.4. Development and statistical fitting of physical impact models

This step of the proposed procedure involves situations in which, because of model availability and the specific minimum requirements set by the user, it is impossible to find a suitable physical impact model for a particular asset class of interest at the screening phase. In this case, suitable methods can be employed to develop the required model based on existing empirical information (i.e., observed damage and/or impact data from past hazard events), synthetic data derived from analytical or numerical models, or expert judgement. After collecting or synthetically generating the required data, statistical approaches are used to fit relevant mathematical functions (see Section 2.1) to the data. The proposed procedure does not involve scoring the developed physical impact models. However, a modelling approach should be selected carefully considering the scoring criteria defined above, emphasising the minimum modelling and user-specific requirements. This Section mainly focuses on empirically- and synthetically-derived functions, with no intention of providing a thorough review of modelling approaches for different assets and hazards. Expert-judgement approaches are briefly discussed at the end.

3.4.1. Model development

Empirical physical impact models require collecting data on previous observations of natural-hazard physical impacts. Sources of these data include post-event surveys conducted by reconnaissance teams or through remote sensing techniques, tax assessor

16

or insurance claims data, and experimental testing. Examples of related datasets include: the GEM earthquake consequence database (GEMECD, last accessed June 2022), the emergency events database (EM-DAT, last accessed June 2022), the USA national oceanic and atmospheric administration (NOAA, last accessed June 2022) database, and earthquake engineering research institute (EERI, last accessed June 2022) reconnaissance data. For each asset in a portfolio, the datasets generally

5 include: 1) the IM level (for fragility and vulnerability); 2) the DS (for fragility and damage-to-impact) and/or the impact (for vulnerability and damage-to-impact); and 3) exposure taxonomy attributes of the assets. Provided enough data is available, empirical models are considered the most credible since they are derived based on actual observations. However, the quality of an empirical database may be jeopardised (e.g., [156]) by the size and/or statistical representativeness of the sample (i.e., sampling errors). The empirical data need to comprise an unbiased (random) collection of observations in each DS (or across

10 all impact values) of interest that are documented using a consistent reporting protocol. These data can be affected by various non-sampling errors, which may involve: under-coverage errors; inaccurate measurements/estimations of the IM [17]; ambiguous definition of DSs; incomplete definition of the asset classes; and inexperience of the survey teams. Rossetto et al. [150] describe these error types in the context of earthquake physical impact modelling. However, empirical models are derived similarly (and the same related challenges are encountered) for any hazard.

15 Synthetic physical impact models are derived from analytical or numerical modelling of the mechanical response of an asset to one or more hazards of interest. The mechanical modelling required depends on the type of mechanical response and, therefore, the specific asset and hazard of interest. The considered asset class is generally represented by one or more archetype (or index) assets (e.g., [157]). These archetypes are characterised in detail by considering the specific geometry (e.g., the height of each pier in a bridge), material properties (e.g., steel yield stress), and relevant structural details (e.g., wall-to-roof

20 connection, relevant for wind fragility). A synthetic model is then generally used to calculate an EDP for a set of hazard loadings with different IM levels. The selected EDP must be representative of the damage levels associated with the considered asset and hazard combination, i.e., it should be possible to associate mechanics-based thresholds of the EDP to different DSs. Different combinations of assets and hazards can produce different damage mechanisms, which are captured to varying degrees by different EDPs. For example, peak EDPs (e.g., maximum displacement, maximum force) tend to be appropriate when the

25 history of the hazard excitation may be disregarded (e.g., single earthquakes, tsunamis, landslides). Cumulative parameters (e.g., number of vibration cycles, hysteretic dissipated energy) are instead more appropriate for capturing progressive damage induced by high-cycle fatigue (e.g., wind-induced vibrations involving a large number of low-amplitude cycles; e.g., [158]) or cumulative damage (e.g., earthquake sequences, earthquake-tsunami sequences, affecting the asset in a pre-damaged condition; e.g., [159]). Using these EDPs may be challenging in practice due to the unavailability of corresponding DS scales (e.g., an

30 earthquake damage scale based on deformation is readily available, while obtaining an energy-based one requires further modelling [159]). For each considered level of IM, the user identifies a set of hazard records to which the asset is subjected (e.g., ground-acceleration time series for earthquakes, velocity and depth time series for tsunami or landslides, wind speed time series), calculates the EDP and estimates the associated DS.

Synthetic models can be used to develop impact data for vulnerability fitting by combining asset-level fragility functions fit

35 using synthetic damage data (see below) with empirical damage-to-impact models (Section 2.1). More refined approaches (e.g., FEMA P58 for earthquakes; [160] combine synthetic analysis response results with pre-determined component-level fragility and vulnerability relationships to produce asset-level vulnerability models. For some hazards, it is not yet possible to model the response and damage physics of each asset component, which means that it is not reasonably simple to estimate EDP values or EDP thresholds that can be linked to different DSs (i.e., EDP-DS relationships). For instance, in the case of

40 floods, different asset components (e.g., a carpet versus industrial machinery) show remarkably different damage mechanisms for a given combination of water depth and flood duration (e.g., carpet damage is related to chemical processes, whereas industrial machinery damage is related to electric/electronic processes), which makes it challenging to define EDP-DS relationships on a component-by-component basis. Nofal and van de Lindt [161] have recently overcome this challenge using empirical data (water depth, flood duration, economic impact) to define component-level DSs by identifying their depth and

45 duration resistance for different DSs (expressed as ranges of economic loss). They then follow a simulation-based approach to develop component-based fragility and vulnerability curves (surfaces), which are subsequently converted to building fragility and vulnerability curves (surfaces).

Expert-judgement-based functions are used in the absence of observed data from past events and/or a combination of computational resources and modelling skills for conducting relevant numerical analyses. These functions can be derived, for

50 instance, using the Delphi Process [162], which requires several experts to provide educated guesses of the damage (or loss)

that would occur to a specific asset class which subjected to a prescribed magnitude of a hazard IM. The judgement can then be weighted according to the expert's experience level to produce a physical impact model. This process requires thoughtful vetting of the participants. It will most likely lead to an underestimation of uncertainty, given the well-known tendency of experts to have overconfidence in their opinions ([156,163], sloanreview.mit.edu/article/managing-overconfidence). The subjectivity of the weightings can also amplify inaccuracies in the models obtained. Due to the above issues, this approach to fitting physical impact models is not recommended for use within the proposed procedure and is not discussed further.

3.4.2. Model fitting

For fragility function fitting, the underlying empirical or synthetic data can be expressed in two different formats, which are broadly classified as "actual" or "bounded" [164]. "Actual" data refers to cases in which an asset has actually reached (or exceeded) the DS of interest at a known value of hazard IM, and are analogous to the results obtained in an incremental dynamic analysis that is used to determine a structure's earthquake collapse capacity [165]. "Bounded" data refers to cases in which only the largest value of hazard intensity reached is known and whether or not the DS of interest was exceeded at (or below) that intensity level, and are comparable to the results obtained using a multiple stripes approach for determining earthquake collapse capacity [165]. On the other hand, empirical or analytically-derived consequence data for vulnerability function and probabilistic damage-to-impact model fitting is continuous (by definition). Across all three data contexts, function fitting can be achieved through a maximum likelihood approach, which -given a prescribed functional form (see Section 2.1) that can be multivariate in the case of vector-valued impact models [74]- computes the corresponding parameters of the model with the highest likelihood of producing the data that were observed. Goodness-of-fit measures (e.g., minimum Akaike information criterion, cross-validation; see [17]) can then be employed to distinguish the best model for the underlying data if several functional forms are available for consideration.

For synthetic derivations of fragility functions, it may be important to consider how the structural response analysis is carried out. For instance, it has been demonstrated [165] that analysing the earthquake collapse probabilities of structures using the multiple stripes approach [166] produces more efficient (site-agnostic) fragility models than those obtained from incremental dynamic analysis [167]. Furthermore, the choice of IMs used in the fragility function is crucial. For instance, Kohrangi et al. [168] found that an IM consisting of a geometric mean of multiple spectral accelerations is relatively more sufficient and produces significantly more efficient earthquake fragility functions than a single-period first-mode spectral acceleration value. A more detailed discussion on challenges and issues to consider with synthetic fragility/vulnerability modelling is found in [42], which specifically refers to earthquakes but is broadly applicable across any hazard context. Empirical data collection challenges and related errors can negatively affect the derivation of empirical physical impact models, for example leading to biased fits (e.g., [156], [17]).

4. Illustrative application: Tomorrowville

4.1. Description of the case study

The proposed methodology to score, select, and develop multi-hazard physical impact models is applied to the virtual urban testbed "Tomorrowville". This synthetic urban area is explicitly designed as a testbed for the TCDSE [169] of the Tomorrow's Cities research programme. Although created fictitiously, Tomorrowville was developed using a digital elevation model of a real location consisting of a 500ha area south of Kathmandu (Nepal). Tomorrowville reflects the typical demographic, socioeconomic and physical features of urban landscapes in the Global South, particularly those of Kathmandu and Nairobi (Kenya). This virtual testbed area is susceptible to earthquakes, floods, and debris flows [170].

Tomorrowville is underpinned by a relational database of spatially-distributed information on its urban features, which is implemented in a GIS environment. The database – described in detail in [171] – includes land-use polygon information, building (physical) attributes, household (social) attributes, and individual/person (social) attributes (note that infrastructure information is yet to be considered). The adopted physical impact models are assigned to buildings in the Tomorrowville GIS database through developed taxonomy strings, which are stored as attributes in the building layer. In addition, a physical impact

table, including the numerical definition of the physical impact model (earthquakes, floods, and debris flows) corresponding to each taxonomy string, is provided in a separate file ("vulnerabilityInventory"). These data are publicly available [172]. Various building layouts have been created for Tomorrowville to explore the risk implications of different urban development options (conditional urban plans) in the context of the TCDSE. These cases are shown in Figure 4, together with the underlying

5   land-use polygons. The first scenario (TV0_b0) refers to the present-day configuration of Tomorrowville. The TV50_total scenario is also considered, representing one possible configuration of Tomorrowville 50 years in the future and including TV0_b0. A detailed description of the exposure layers in Tomorrowville is considered out of the scope of this paper (but available in [171]), which will only discuss the definition of the building classes related to physical impact characterisation.
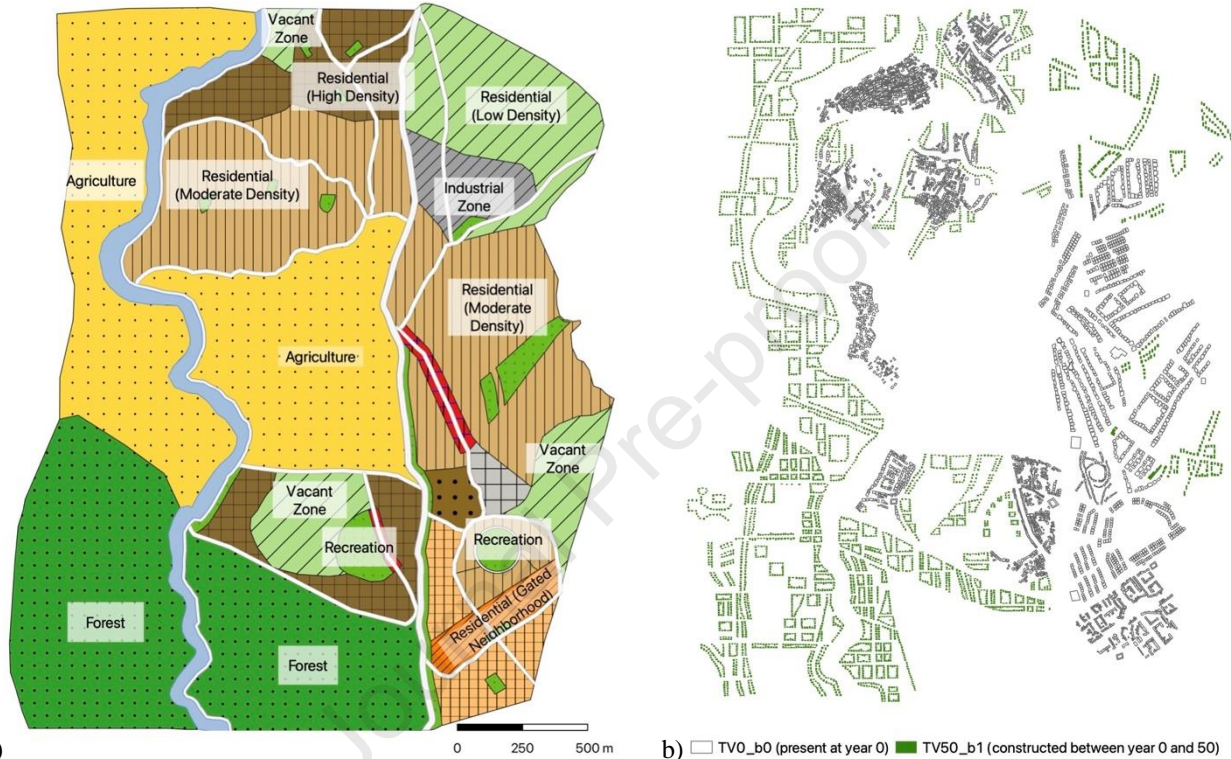

10   a)

Figure 4 Tomorrowville: a) land-use polygons (adapted from [172]); b) TV50_total.

4.2. Exposure characterisation (preliminary phase of the procedure)

TV0_b0 contains 4,810 buildings (stored in the layer "buildingsTV0"). The building attributes are generated algorithmically to be consistent with relevant statistical distributions of Nairobi and Kathmandu building data [171]. However, the lack of

15   detailed data available for this case study means that it is only possible to characterise a subset of the GED4ALL attributes affecting physical impact modelling for the considered hazards (see Table 1): occupancy type, building material, lateral resisting system, height and code level. Each combination of occupancy type, building material, lateral resisting system, height and code level constitutes a building class within Tomorrowville, which is mapped to a set of relevant physical impact models related to earthquakes, floods, and debris flows using GED4ALL taxonomy strings. Ad-hoc simplified taxonomy strings are

20   also defined to simplify communication among stakeholders and researchers of different backgrounds during the interdisciplinary data-generation process for Tomorrowville.

As discussed in the previous sections, different attributes are relevant for physical impact models of different hazards. Table 5 shows the values adopted for the different taxonomy attributes, including their labelling according to both GED4ALL and the simplified ad-hoc taxonomy strings. Note that the simplified taxonomy strings are discussed herein for simplicity.

19

Ordinary buildings in Tomorrowville are generally classified as residential (Res), commercial (Com), or industrial (Ind). Schools and hospitals also feature in Tomorrowville. For this application, the occupancy type only affects the flood and debris flow vulnerability models, together with the construction material and the number of storeys.

5   The possible combinations of building material and lateral load resisting system parameters within Tomorrowville are adobe wall buildings (Adb), informal settlements in stone and mud (StMin), brick and mud wall buildings (BrM), brick and cement walls with flexible floor slabs (BrCfl), brick and cement walls with rigid floor slabs (BrCri) and masonry-infilled reinforced concrete frames (RCi). The StMin buildings can be either one- or two-storey tall, while the Adb, BrM, BrCi, BrCfl buildings can reach up to four storeys. Finally, the height of the RCi buildings ranges between one and eight storeys. Considering the physical impact models used for this application (see Section 4.4), the material affects earthquake, flood and debris flow

10 models while the lateral resisting system affects earthquake models only.

Building design codes associated with building classes in Tomorrowville (which only affect earthquake physical impact models in this case) are defined based on the evolution of seismic design codes in Nepal: low-code (LC) buildings are designed without any seismic code provisions; moderate-code (MC) buildings refer to construction practices in the period 1994-2015, and are therefore assumed to be compliant with the NBC1994 code (Nepal national building code, [173]); high-code (HC)

15 buildings are assumed to be compliant with the NBC2015 code [173], and designed with higher risk awareness of the designers after the 2015 earthquake in Nepal. RCi buildings can be assigned any of the above codes, while all other building types are low code due to poor code compliance that is assumed to be prevalent in the considered case-study area. Each land-use polygon within the TV0_b0 scenario is associated with a specific distribution of the above parameters (see [171] for details). The occupancy type of buildings in each polygon (Figure 5a) depends on the underlying land use (e.g., residential, commercial,

20 etc.). Figure 5b displays the material and lateral resisting system combination for each building. Reinforced concrete frames with masonry infills (RCi) constitute approximately 62% of the buildings within the "commercial and residential", "industrial", "city centre", and "high income" land-use polygons, and approximately 40% of buildings within the "historical preservation" and the "middle income" polygons. BrM is predominant (i.e., represents 66% of buildings) in the "agriculture" and "low-income" polygons. Proportions of other combinations of material and lateral resisting systems are approximately uniform

25 across all polygon types, ranging from 1% to 7%. As seen in Figure 5c, most buildings in TV0_b0 are low rise (i.e., LR, between one and four storeys), and less than 20% of all reinforced concrete buildings are mid-rise (i.e., MR, between five and seven storeys). Finally, the proportion of different code design levels (Figure 5d) depends on the polygon type. Notably, 70% of RCi buildings are low code in the low-income polygons, 60% are moderate code in middle-income polygons, and 70% are high code in high-income polygons. The distribution of occupancy type, height and code level of buildings in the TV50_total

30 layer follows the corresponding assumptions adopted for TV0_b0.

Table 5 Adopted exposure taxonomy attributes, considering the GED4ALL and the simplified ad-hoc taxonomies.

Attributes	Values	Label (simplified taxonomy)	Label (GED4ALL taxonomy)
Occupancy	Residential	Res	RES
	Commercial	Com	COM
	Industrial	Ind	IND
Material +	adobe walls	Adb	MUR+ADO/LWAL
lateral resisting system +	stone and mud (informal settlements)	StMin	MUR+ST+MOM/LWAL
	brick and mud walls	BrM	MUR+CL+MOM/LWAL
	brick and cement walls with flexible floor slabs	BrCfl	MUR+CLBRS+MOC/LWAL/--FWCN
	brick and cement walls with rigid floor slabs	BrCri	MUR+ CLBRS+MOC/LWAL/--FWCN
	masonry-infilled reinforced concrete frames	RCi	CR+CIP/LFINF
Date of construction	Pre 1994 (Low code)	LC	YPRE:1994 (and LFINF+CDL)
(proxy for code level)	Between 1994 and 2015	MC	YBET:1994:2015 (and LFINF+CDM)
	After 205	HC	YBET:2016:2022 (also LFINF+CDH)
Height	1-8 storeys	1s-8s	H:1-H:8
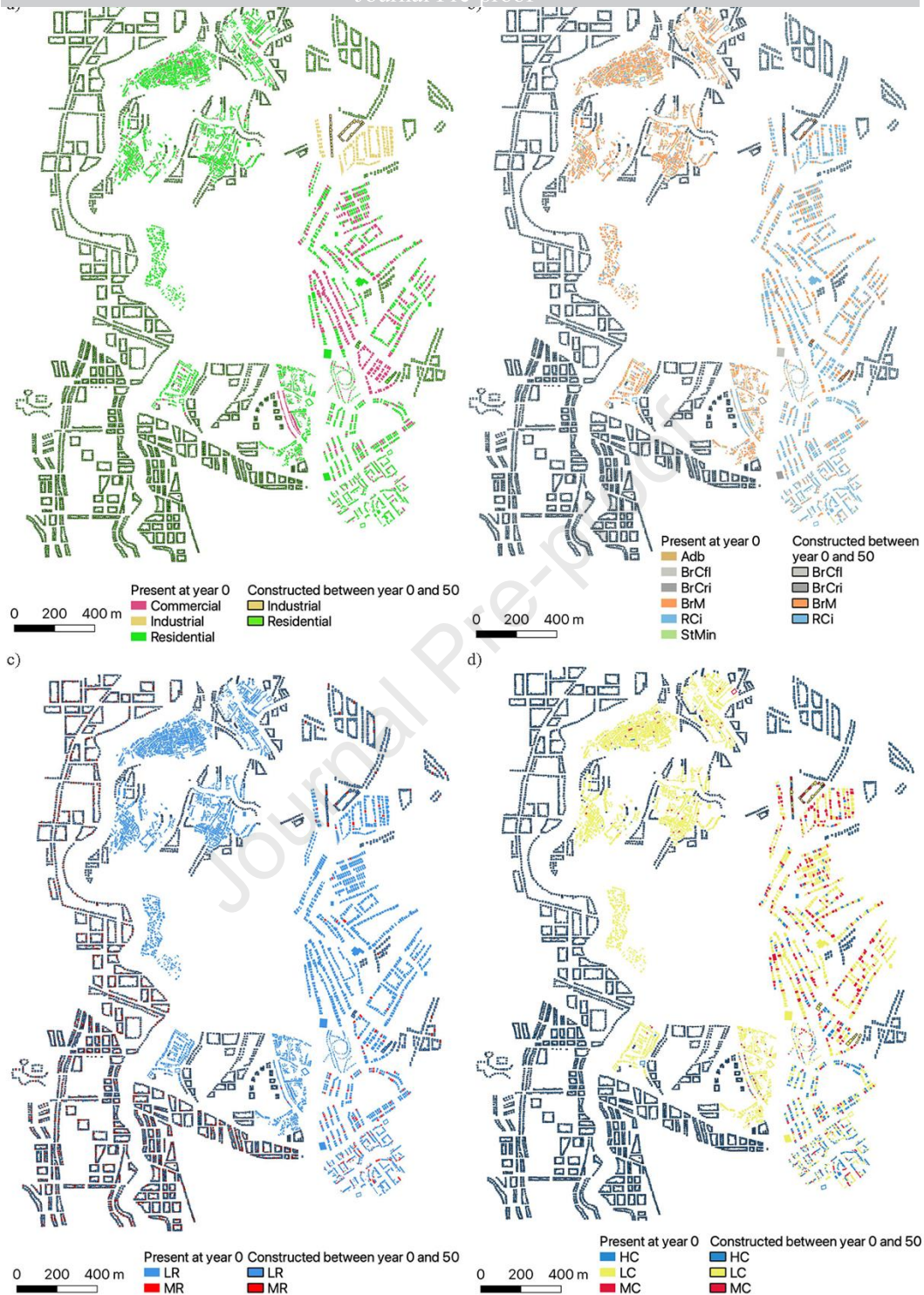
Figure 5 Building-class attributes of the TV50_total scenario in Tomorroville: a) occupancy type; b) material and lateral resisting system; c) height; d) code level.

4.3. Modelling choices and user requirements for the procedure

The selected hazards for Tomorrowville are earthquakes, floods, and debris flows. For the specific application of the TCDSE to Tomorrowille and the particular "physical infrastructure impact" module of the TCDSE related to this work, fragility models are generally preferred – whenever available – over vulnerability models, since estimating damage enables greater flexibility in subsequently characterising a wide array of impact metrics (e.g., casualties, human displacement) that may also draw on social information as part of the ensuing "social impact" module.

Kathmandu is the considered location when applying the proposed procedure since the physical geographical representation of Tomorrowville (including a digital elevation model) was derived from the Kathmandu Valley. For this specific case study area, it is reasonably assumed that flood physical impact models can also capture debris-flow impacts; the low flow velocities and sediment concentration of debris flows within the shallow topography of building locations on the valley floor means that damage is principally caused by inundation, rather than hydrodynamic stress and impacts from debris [170]. Moreover, since the damage mechanism due to earthquakes (mainly displacement-related damage) is unrelated to the damage due to floods/debris flows, the physical impact models of the building classes in Tomorrowville are considered independent, such that no multi-hazard fragility interaction is considered. Time-dependent physical impact is also not explicitly considered for simplicity. However, it can be approximately facilitated by scaling the parameters of the adopted physical impact models (e.g., [3]) using properly-calibrated factors (e.g., reducing the medians of a set of fragility functions).

The most important user-specific model requirement for this application involves preferring sets of asset class-specific models (e.g., explicitly capturing the plastic mechanisms of a class) that are derived using consistent assumptions and modelling techniques and that can cover multiple asset classes within Tomorrowville. Selecting consistently-derived models maximises the consistency of the damage estimations within the risk model. Models using advanced IMs are also preferred over models adopting more-conventional IMs.

Finally, the adopted weights for TOPSIS are respectively equal to 25%, 15%, 40%, and 20% for the relevance, statistical refinement, model quality, and user requirements criteria respectively. The numerical values assigned to the low, medium, and high scores for the criteria are, 1, 2, and 3 respectively. This specific implementation of TOPSIS is available at github.com/robgen/rankFragilityVulnerability (last accessed June 2022).

4.4. Selected physical impact models

This section provides an overview of the selected physical impact models for all building classes within Tomorrowville. The proposed procedure is described in detail for an example building class (summarised in Table 6 and Figure 6), namely RCi+MC+6s+Res in the simplified taxonomy and CR+CIP/LFINF+CDM/H:6/YBET:1994:2015 according to GED4ALL. Among the available databases mentioned in Section 3.2.1 (point 2 of the screening phase) for earthquakes, the GEM vulnerability and the European seismic risk model databases only produced three candidate models: Akkar et al. [174], Erberik [175], and CR_LFINF_CDM-0_H6 in Crowley et al. [131]. The first two models are based on a numerical approach involving single degree of freedom representation of the structures and refer to residential reinforced concrete buildings in Turkey, which are broadly classified as "Asia" models within the GEM database. The third model is based on a similar methodology and refers to residential masonry-infilled concrete frame European buildings with moderate code provisions.

Among the model compendia mentioned in Section 3.2.2 (point 3 of the screening procedure) for earthquakes, Rossetto et al. [138] produced the same candidate models as the GEM interactive database, while Calvi et al. [139] produced no matches. The HAZUS earthquake fragility model for mid-rise, moderate code reinforced concrete frames is a further match produced in this procedure step. Even though it refers explicitly to USA building classes, it is considered because it is commonly used for other regions. Moreover, as demonstrated elsewhere (e.g., [176,177]), mapping the seismic design codes of Global South countries against the historical evolution of USA design codes is fairly straightforward. A literature review specifically tailored to Nepali building classes (point 4 of the screening procedure) returned the model by Gautam et al. [178] as an output. This empirical model is derived from a large dataset of IM vs damage compiled in the aftermath of five major Nepali earthquakes. The literature review was continued by relaxing the constraint on the geographical location (i.e., targeting generic reinforced concrete building classes) but including some specific model requirements (used as a criterion in the scoring phase), particularly the explicit consideration of the building plastic mechanism (indirectly related to the level of seismic code), and the use of advanced IMs. The result of this search is the study by Gentile and Galasso [179], which provides fragility models

for generic masonry-infilled reinforced concrete frames for relevant combinations of height and plastic mechanisms specifically tailored to different design code levels. The Gentile and Galasso models cover all the relevant concrete building classes in Tomorrowville. This means that multiple building classes are associated with models generated from the same methodology and assumptions, maximising the consistency of the damage estimations in the risk model as far as possible (which is one specific model requirement for this application). Finally, these models adopt the geometric mean of the spectral acceleration across a range of periods, which is an advanced IM.

All the identified earthquake candidate models passed point 5 of the screening phase since they include adequate documentation (associated with international journal papers), an adequate damage scale covering four DSs, and require no IM extrapolation for their specific use in Tomorrowville. The candidate models are then scored against the scoring criteria, as shown in Table 6. Although scoring only "medium" for "relevance", the model by Gentile and Galasso, shown in Figure 6a, was selected since it scored "high" in all other criteria, finally resulting in a higher overall score according to TOPSIS (Table 6).

For floods (and debris flows), the only available interactive database to perform a search according to point 2 of the procedure is the flood model database (see Section 3.2.1). A search within this database only produces the JRC, Asia, Concrete, and Residential empirical vulnerability function as a candidate model. The model compendia search supporting point 3 of the procedure results in the same model as well as the HAZUS, six-storey, Concrete, Residential model. The JRC vulnerability functions are defined starting from the three JRC baseline Asia functions for residential, commercial, and industrial buildings, and then a loss multiplier is applied based on construction material (equal to 0.6 for concrete). Note that this model can be consistently applied to all building classes in Tomorrowville, which is one of the selected user requirements. A literature review specifically tailored to Nepali building classes did not produce any relevant match. For completeness, the empirical model in [180] for Thailand is herein mentioned as the country-level model closest to the geographic area relevant for Tomorrowville. According to the above features, the candidate flood models are scored against the criteria and ranked according to TOPSIS (Table 6). The JRC model (shown in Figure 6b) was selected due to its higher score in the "relevance" criterion.

Table 6 Model scoring for the CR+CIP/LFINF+CDM/H:6/YBET:1994:2015 (RCi+MC+6s+Res) building class. The score for each criterion is underlined

Criterion: Attribute	Earthquake						Flood and debris flow		
	Akkar	Erberik	Crowley	HAZUS	Gautam	Gentile	JRC	HAZUS	Tang
Relevance:									
Geographical area	Low	Low	Low	Low	High	Med	Med	Low	Low
Asset characteristics	Med	Med	Med	Low	Med	High	Med	Med	Med
IM	Med	Med	Med	Low	Med	High	High	High	High
Statistical refinement:									
Uncertainties	Med	Med	Med	Med	Med	High	Med	Med	Med
First principles	High	High	High	High	High	High	High	High	High
Model quality (empirical):									
Impact observations	-	-	-	-	-	-	Med	Med	Med
IM observations	-	-	-	-	-	-	High	High	High
Constrained asset class	-	-	-	-	-	-	Med	Med	Low
Data quantity	-	-	-	-	-	-	High	High	Med
Model quality (synthetic):									
Fidelity to mechanics	Med	Med	Med	Med	Med	High	-	-	-
Aggregation level	Med	Med	Med	Med	High	High	-	-	-
User requirements	Med	Med	Med	Med	Med	High	Low	Low	Low
TOPSIS score	0	0	0	0	0.55	0.66	1	0.60	0
Ranking	**3**	**3**	**3**	**3**	**2**	**1**	**1**	**2**	**3**

23

The JRC vulnerability models depend on an assumed total building value. This is set to 1 for each considered building class in Tomorrowville to normalise losses, providing a proxy for damage (consistent with the damage output from the implemented earthquake fragility functions). The JRC vulnerability curves do not vary as a function of building height; therefore, they ranked "medium" in the "constrained asset class" attribute. An ad-hoc height modifier is developed in this study to overcome this limitation. This modifier is based on the assumption that the JRC functions are valid for buildings of a given reference number of storeys (n_{ref}), which is the average number of storeys within the JRC dataset (herein considered equal to 2). This modifier also assumes that the absolute value of flood loss for a given building class only depends on the flood depth, $L(h_w)$, and is independent of the building height (i.e., the loss can only be caused by damaged contents present in inundated storeys). This condition is expressed in Eq. 5, where LR is the loss normalised by the total reconstruction cost RC (note that the subscripts "bld" and "ref" respectively refer to a generic and the reference-height building). The total reconstruction cost of a building within a given class is assumed to be linearly proportional to the number of storeys ($RC_{bld} = n_{bld}rc$, in which n_{bld} is the number of storeys of the building, and rc is the reconstruction cost of one storey). By substituting this last equation into Eq. 5, one can obtain the height-modified normalised loss (Eq. 6). This calculation is capped at LR = 1, whenever appropriate. Figure 6b shows the height-modified vulnerability curve developed for the RCi+6s+Res class as an example.

$$L_{ref}(h_w) = L_{bld}(h_w) \xrightarrow{yields} LR_{ref}(h_w)RC_{ref} = LR_{bld}(h_w)RC_{bld} \qquad 5$$

$$LR_{bld}(h_w) = \frac{n_{ref}}{n_{bld}}LR_{ref}(h_w) \qquad 6$$
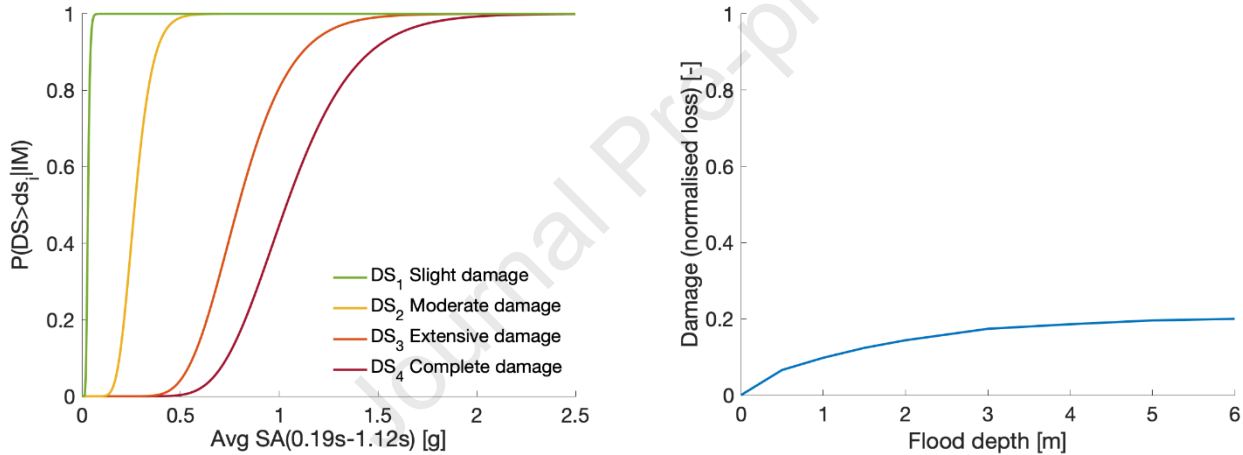
Figure 6 Six-storey masonry-infilled reinforced concrete building (CR+CIP/LFINF+CDM/H:6/YBET:1994:2015 or RCi+MC+6s+Res): a) earthquake fragility functions; b) flood/debris flow vulnerability functions. Note that a 6m flood causes a ~20% loss because it only affects approximately two storeys.

After applying the model selection procedure to all the building classes in Tomorrowville, 11 different earthquake fragility models are deemed necessary. The fragility models in the study by Guragain [181] calibrated explicitly on Nepalese building classes, are selected and applied based on the Adb, BrM, BrCfl, BrCri, StMin components of the taxonomy string. All of these models have been derived from the same numerical modelling approach, leading to consistent damage estimations for the underlying building classes and ultimately enhanced consistency in the risk model itself. The IM used in these models is either peak ground acceleration (BrM, BrCfl, BrCri), or spectral acceleration at the structure's fundamental period, considered equal to 0.3s (Adb, StMin). The earthquake fragility models proposed in [182] are used for all the RCi buildings, and are assigned based on height (LR, MR) and code-level (LC, MC, HC) components of the taxonomy string; six different RCi building classes (i.e, combinations of LR/MR and LC/MC/HC) are present in the Tomorrowville conditional urban plans. All of the adopted earthquake fragility models are based on numerical simulations and use the same DS characterisation, i.e., slight (DS1), moderate (DS2), extensive (DS3), and complete (DS4).

24

The JRC model is applied to all the building classes in Tomorrowville, considering the "Asia, Res" baseline function. According to the JRC guidelines, the maximum damage of the baseline functions is multiplied by factors equal to 0.6 for RCi buildings, 1 for Adb, BrM, BrCfl, BrCri buildings, and 0.075 for StMin buildings. The height modifier of equations 5 and 6 is then applied, leading to 48 unique flood/debris-flow vulnerability functions across all considered building classes.

5. Conclusions

This paper has described a structured methodology for characterising the multi-hazard physical impact modelling of a portfolio of assets across an urban system. Given a set of relevant hazards for any selected case-study region, the methodology involves 1) mapping the relevant asset classes (i.e. construction types) in a considered area to a set of existing candidate fragility, vulnerability, and/or damage-to-impact models, also accounting for any specific modelling requirements (e.g., models with consistent assumptions valid for multiple classes, time dependency, multi-hazard interaction); 2) scoring the candidate models according to relevant criteria to select the most suitable ones; or 3) using state-of-the-art numerical and/or empirical methods to develop fragility/vulnerability models not already available, supplementing existing models.

The proposed methodology is applied to the virtual testbed "Tomorrowville", a synthetic-but-realistic urban area specifically designed as a testbed for the Tomorrow's Cities Decision Support Environment. Tomorrowville reflects the typical demographic, socioeconomic and physical features of urban landscapes in the Global South and is susceptible to earthquakes, floods, and debris flows.

The main goal of this procedure is to provide a framework that facilitates the consistent selection of a set of candidate physical impact models to use within risk modelling applications. This selection is based on a rigorous evaluation that considers criteria related to the accuracy, computational complexity, data requirements, and specific user requirements of a risk model. Future repeated applications of the procedure will allow a refinement of the suggested values for all the relevant input parameters (e.g., specific criteria, threshold values for screening, scoring schemes, and weights). The proposed methodology facilitates effective characterisation of the multi-hazard, time-dependent physical impact modelling of a portfolio of assets, which is particularly useful in future-looking (risk-informed urban planning) contexts.

Acknowledgements

References

[1]   U.N. Secretary general, Report of the open-ended intergovernmental expert working group on indicators and terminology relating to disaster risk reduction. Proceedings of the Seventy-First Session Agenda, Item 19, 2016.

[2]   G. Limongi, A. Galderisi, Twenty years of European and international research on vulnerability: A multi-faceted concept for better dealing with evolving risk landscapes, International Journal of Disaster Risk Reduction. 63 (2021) 102451. https://doi.org/10.1016/j.ijdrr.2021.102451.

[3]   G. Cremen, C. Galasso, J. McCloskey, A Simulation-Based Framework for Earthquake Risk-Informed and People-Centered Decision Making on Future Urban Planning, Earths Future. 10 (2022). https://doi.org/10.1029/2021EF002388.

[4]   G. Cremen, E.Y. Mentese, M.E. Filippi, R. Gentile, C. Galasso, J. McCloskey, A State-of-the-Art Environment for Supporting Risk-Sensitive Decisions on Urbanisation in Tomorrow's Cities, International Journal of Disaster Risk Reduction. under rev (2022).

[5]   C. Mesta, G. Cremen, C. Galasso, Urban growth modelling and social vulnerability assessment for a hazardous Kathmandu Valley, Sci Rep. 12 (2022) 6152. https://doi.org/10.1038/s41598-022-09347-x.

[6]   A. Calderón, V. Silva, Exposure forecasting for seismic risk estimation. Application to Costa Rica, Earthquake Spectra. 37 (2021) 1806–1826. https://doi.org/10.1177/8755293021989333.

[7]   E. Bastidas-Arteaga, M.G. Stewar, Climate Adaptation Engineering, Elsevier, 2019. https://doi.org/10.1016/C2017-0-00942-4.

[8]   G.A. Riddell, H. van Delden, H.R. Maier, A.C. Zecchin, Tomorrow's disasters – Embedding foresight principles into disaster risk assessment and treatment, International Journal of Disaster Risk Reduction. 45 (2020) 101437. https://doi.org/10.1016/j.ijdrr.2019.101437.

[9]   E.Y. Mentese, G. Cremen, R. Gentile, M.E. Filippi, C. Galasso, J. McCloskey, Risk-Informed Urbanisation Scenario Development through Interdisciplinary and GIS-Based Processes, International Journal of Disaster Risk Reduction. under rev (2022).

[10]   G. Cremen, E.Y. Mentese, M.E. Filippi, R. Gentile, C. Galasso, J. McCloskey, A State-of-the-Art Environment for Supporting Risk-Sensitive Decisions on Urbanisation in Tomorrow's Cities, International Journal of Disaster Risk Reduction. under rev (2022).

[11]   M.E. Filippi, A. Barcena, R. Šakić Trogrlić, G. Cremen, E.Y. Mentese, R. Gentile, L. Jenkins, D.P. Poudel, M.J. Creed, V. Manandhar, J. McCloskey, M. Rai, S. Adhikari, M. Muthusamy, C. Galasso, Interdisciplinarity in practice: reflections from early career researchers developing a risk-informed decision support environment for Tomorrow's Cities, International Journal of Disaster Risk Reduction. under rev (2022).

[12]   L.T. Jenkins, M. Creed, K. Tarbali, M. Muthusamy, robert sakic Trogrlic, J. Philips, S. Watson, H. Sinclair, C. Galasso, J. McCloskey, Physics-based simulations of multiple natural hazards for risk sensitive land use planning in expanding urban regions undefined, International Journal of Disaster Risk Reduction. under rev (2022).

[13]   H. Ebrahimian, F. Jalayer, Selection of seismic intensity measures for prescribed limit states using alternative nonlinear dynamic analysis methods, Earthq Eng Struct Dyn. 50 (2021) 1235–1250. https://doi.org/10.1002/eqe.3393.

[14]   C. Tarbotton, F. Dall'Osso, D. Dominey-Howes, J. Goff, The use of empirical vulnerability functions to assess the response of buildings to tsunami impact: Comparative review and summary of best practice, Earth Sci Rev. 142 (2015) 120–134. https://doi.org/10.1016/j.earscirev.2015.01.002.

[15]   G. Cremen, J.W. Baker, Improving FEMA P-58 non-structural component fragility functions and loss predictions, Bulletin of Earthquake Engineering. 17 (2019) 1941–1960. https://doi.org/10.1007/s10518-018-00535-7.

[16]   T. Rossetto, I. Ioannu, D. Grant, T. Maqsood, Guidelines for empirical vulnerability assessment, 2014.

[17]   D. Lallemant, A. Kiremidjian, H. Burton, Statistical procedures for developing earthquake damage fragility curves, Earthq Eng Struct Dyn. 44 (2015) 1373–1389. https://doi.org/10.1002/eqe.2522.

[18]   F. Jalayer, R. de Risi, G. Manfredi, Bayesian Cloud Analysis: efficient structural fragility assessment using linear regression, Bulletin of Earthquake Engineering. 13 (2015) 1183–1203.

[19]   M. Nguyen, D. Lallemant, Order Matters: The Benefits of Ordinal Fragility Curves for Damage and Loss Estimation, Risk Analysis. (2021). https://doi.org/10.1111/risa.13815.

[20]   V. Silva, H. Crowley, H. Varum, R. Pinho, L. Sousa, Investigation of the characteristics of Portuguese regular moment-frame RC buildings and development of a vulnerability model, Bulletin of Earthquake Engineering. 13 (2015) 1455–1490. https://doi.org/10.1007/s10518-014-9669-y.

[21]   D. Lallemant, A. Kiremidjian, A Beta Distribution Model for Characterizing Earthquake Damage State Distribution, Earthquake Spectra. 31 (2015) 1337–1352. https://doi.org/10.1193/012413EQS013M.

[22]   F. Carisi, K. Schröter, A. Domeneghetti, H. Kreibich, A. Castellarin, Development and assessment of uni- and multivariable flood loss models for Emilia-Romagna (Italy), Natural Hazards and Earth System Sciences. 18 (2018) 2057–2079. https://doi.org/10.5194/nhess-18-2057-2018.

[23]   E. Martínez-Gomariz, E. Forero-Ortiz, M. Guerrero-Hidalga, S. Castán, M. Gómez, Flood Depth–Damage Curves for Spanish Urban Areas, Sustainability. 12 (2020) 2666. https://doi.org/10.3390/su12072666.

[24]   R. Figueiredo, X. Romão, E. Paupério, Component-based flood vulnerability modelling for cultural heritage buildings, International Journal of Disaster Risk Reduction. 61 (2021) 102323. https://doi.org/10.1016/j.ijdrr.2021.102323.

[25]   S. Lagomarsino, S. Giovinazzi, Macroseismic and mechanical models for the vulnerability and damage assessment of current buildings, Bulletin of Earthquake Engineering. (2006). https://doi.org/10.1007/s10518-006-9024-z.

[26] L. Martins, V. Silva, M. Marques, H. Crowley, R. Delgado, Development and assessment of damage-to-loss models for moment-frame reinforced concrete buildings, Earthq Eng Struct Dyn. 45 (2016) 797–817. https://doi.org/10.1002/eqe.2687 Development.

[27] L. Martins, V. Silva, M. Marques, H. Crowley, R. Delgado, Development and assessment of damage-to-loss models for moment-frame reinforced concrete buildings, Earthq Eng Struct Dyn. 45 (2016) 797–817. https://doi.org/10.1002/eqe.2687.

[28] Federal Emergency Management Agency, HAZUS MH MR5. Earthquake loss estimation methodology, Washington DC, USA, 2021. https://www.hsdl.org/?view&did=12756.

[29] D.A. Reed, C.J. Friedland, S. Wang, C.C. Massarra, Multi-hazard system-level logit fragility functions, Eng Struct. 122 (2016) 14–23. https://doi.org/10.1016/j.engstruct.2016.05.006.

[30] Y. Li, R. Song, J.W. van de Lindt, Collapse Fragility of Steel Structures Subjected to Earthquake Mainshock-Aftershock Sequences, Journal of Structural Engineering. 140 (2014) 04014095. https://doi.org/10.1061/(ASCE)ST.1943-541X.0001019.

[31] X. Ming, Q. Liang, R. Dawson, X. Xia, J. Hou, A quantitative multi-hazard risk assessment framework for compound flooding considering hazard inter-dependencies and interactions, J Hydrol (Amst). 607 (2022) 127477. https://doi.org/10.1016/j.jhydrol.2022.127477.

[32] P. Gehl, D.M. Seyedi, J. Douglas, Vector-valued fragility functions for seismic risk evaluation, Bulletin of Earthquake Engineering. 11 (2013) 365–384. https://doi.org/10.1007/s10518-012-9402-7.

[33] I. Zentner, A general framework for the estimation of analytical fragility functions based on multivariate probability distributions, Structural Safety. 64 (2017) 54–61. https://doi.org/10.1016/j.strusafe.2016.09.003.

[34] K. Aljawhari, R. Gentile, F. Freddi, C. Galasso, Effects of ground-motion sequences on fragility and vulnerability of case-study reinforced concrete frames, Bulletin of Earthquake Engineering. 19 (2021) 6329–6359. https://doi.org/10.1007/s10518-020-01006-8.

[35] K.H. Lee, D. v. Rosowsky, Fragility analysis of woodframe buildings considering combined snow and earthquake loading, Structural Safety. 28 (2006) 289–303. https://doi.org/10.1016/j.strusafe.2005.08.002.

[36] K. Otárola, J. Fayaz, C. Galasso, Fragility and vulnerability analysis of deteriorating ordinary bridges using simulated ground-motion sequences, Earthq Eng Struct Dyn. under rev (2022).

[37] J. Ghosh, J.E. Padgett, Aging Considerations in the Development of Time-Dependent Seismic Fragility Curves, Journal of Structural Engineering. 136 (2010) 1497–1511. https://doi.org/10.1061/(ASCE)ST.1943-541X.0000260.

[38] X. Ming, W. Xu, Y. Li, J. Du, B. Liu, P. Shi, Quantitative multi-hazard risk assessment with vulnerability surface and hazard joint return period, Stochastic Environmental Research and Risk Assessment. 29 (2015) 35–44. https://doi.org/10.1007/s00477-014-0935-y.

[39] I. Zentner, M. Gündel, N. Bonfils, Fragility analysis methods: Review of existing approaches and application, Nuclear Engineering and Design. 323 (2017) 245–258. https://doi.org/10.1016/j.nucengdes.2016.12.021.

[40] N. Luco, C.A. Cornell, Structure-Specific Scalar Intensity Measures for Near-Source and Ordinary Earthquake Ground Motions, Earthquake Spectra. 23 (2007) 357–392. https://doi.org/10.1193/1.2723158.

[41] A.C. Cornell, Does Duration Really Matter?, in: FHWA/NCEER Workshop on the National Representation of Seismic Ground Motion for New and Existing Highway Facilities, n.d.

[42] V. Silva, S. Akkar, J. Baker, P. Bazzurro, J.M. Castro, H. Crowley, M. Dolsek, C. Galasso, S. Lagomarsino, R. Monteiro, D. Perrone, K. Pitilakis, D. Vamvatsikos, Current challenges and future trends in analytical fragility and vulnerability modeling, Earthquake Spectra. 35 (2019) 1927–1952. https://doi.org/10.1193/042418EQS101O.

[43] Federal Emergency Management Agency, HAZUS - MH MR4 technical manual, Washington DC, USA, 2003.

[44] G. Di Pasquale, G. Orsini, R.W. Romeo, New developments in seismic risk assessment in Italy, Bulletin of Earthquake Engineering. 3 (2005) 101–128. https://doi.org/10.1007/s10518-005-0202-1.

[45] L. Martins, V. Silva, Development of a fragility and vulnerability model for global seismic risk analyses, Bulletin of Earthquake Engineering. 19 (2021) 6719–6745. https://doi.org/10.1007/s10518-020-00885-1.

[46] H.-Y. Noh, A. Kiremidjian, L. Ceferino, E. So, Bayesian Updating of Earthquake Vulnerability Functions with Application to Mortality Rates, Earthquake Spectra. 33 (2017) 1173–1189. https://doi.org/10.1193/081216eqs133m.

[47] F.M. Al-Nammari, M.K. Lindell, Earthquake recovery of historic buildings: exploring cost and time needs, Disasters. 33 (2009) 457–481. https://doi.org/10.1111/j.1467-7717.2008.01083.x.

[48]   D.N. Grant, A mathematical form of probabilistic vulnerability model for loss and casualty ratios, Earthquake Spectra. 36 (2020) 700–717. https://doi.org/10.1177/8755293019891719.

[49]   M. Caruso, R. Pinho, F. Bianchi, F. Cavalieri, M.T. Lemmo, Integrated economic and environmental building classification and optimal seismic vulnerability/energy efficiency retrofitting, Bulletin of Earthquake Engineering. 19 (2021) 3627–3670. https://doi.org/10.1007/s10518-021-01101-4.

[50]   D. Shrestha, D.B. Basnyat, J. Gyawali, M. Creed, H. Sinclair, B. Golding, M. Manoranjan, S. Shrestha, D. Subedi, R. Haiju, Rainfall extremes under future climate change with implications for urban flood risk in Kathmandu, Nepal, International Journal of Disaster Risk Reduction. (2022).

[51]   A. Ali, N. Raut, Advances and Challenges in Flash Flood Risk Assessment: A Review , Article in Journal of Geography & Natural Disasters. 7 (2017). https://doi.org/10.4172/2167-0587.1000195.

[52]   J. Douvinet, D. Delahaye, P. Langlois, Measuring surface flow concentrations using a cellular automaton metric: a new way of detecting potential impacts of flash floods in sedimentary context, Http://Journals.Openedition.Org/Geomorphologie. (2013) 27–46. https://doi.org/10.4000/GEOMORPHOLOGIE.10112.

[53]   D.M. Cruden, D.J. Varnes, Landslides types and processes, Landslides: Investigation and Mitigation, Special Report, 247, Transportation Research Board, National Research Council, Washington DC, 1996.

[54]   E.D. Haugen, A.M. Kaynia, Vulnerability of structures impacted by debris flow, (2008). https://doi.org/10.1201/9780203885284-c37.

[55]   D.H. Peregrine, WATER-WAVE IMPACT ON WALLS, Http://Dx.Doi.Org/10.1146/Annurev.Fluid.35.101101.161153. 35 (2003) 23–43. https://doi.org/10.1146/ANNUREV.FLUID.35.101101.161153.

[56]   O. Hungr, G.C. Morgan, R. Kellerhals, Quantitative analysis of debris torrent hazards for design of remedial measures, Https://Doi.Org/10.1139/T84-073. 21 (1984) 663–677. https://doi.org/10.1139/T84-073.

[57]   M. Jakob, D. Stein, M. Ulmi, Vulnerability of buildings to debris flow impact, Natural Hazards. 60 (2012) 241–261. https://doi.org/10.1007/S11069-011-0007-2/FIGURES/5.

[58]   H.Y. Luo, R.L. Fan, H.J. Wang, L.M. Zhang, Physics of building vulnerability to debris flows, floods and earth flows, Eng Geol. 271 (2020) 105611. https://doi.org/10.1016/J.ENGGEO.2020.105611.

[59]   E. Martínez-Gomariz, E. Forero-Ortiz, M. Guerrero-Hidalga, S. Castán, M. Gómez, Flood Depth–Damage Curves for Spanish Urban Areas, Sustainability. 12 (2020) 2666. https://doi.org/10.3390/su12072666.

[60]   J.W. van de Lindt, M. Taggart, Fragility Analysis Methodology for Performance-Based Analysis of Wood-Frame Buildings for Flood, Nat Hazards Rev. 10 (2009) 113–123. https://doi.org/10.1061/(ASCE)1527-6988(2009)10:3(113).

[61]   O.M. Nofal, J.W. van de Lindt, Understanding flood risk in the context of community resilience modeling for the built environment: research needs and trends, Sustain Resilient Infrastruct. 7 (2022) 171–187. https://doi.org/10.1080/23789689.2020.1722546.

[62]   K. Schröter, H. Kreibich, K. Vogel, C. Riggelsen, F. Scherbaum, B. Merz, How useful are complex flood damage models?, Water Resour Res. 50 (2014) 3378–3395. https://doi.org/10.1002/2013WR014396.

[63]   F. Elmer, A.H. Thieken, I. Pech, H. Kreibich, Influence of flood frequency on residential building losses, Natural Hazards and Earth System Sciences. 10 (2010) 2145–2159. https://doi.org/10.5194/nhess-10-2145-2010.

[64]   F. Parisi, G. Sabella, Flow-type landslide fragility of reinforced concrete framed buildings, Eng Struct. 131 (2017) 28–43. https://doi.org/10.1016/J.ENGSTRUCT.2016.10.013.

[65]   J.A. Prieto, M. Journeay, A.B. Acevedo, J.D. Arbelaez, M. Ulmi, Development of structural debris flow fragility curves (debris flow buildings resistance) using momentum flux rate as a hazard parameter, Eng Geol. 239 (2018) 144–157. https://doi.org/10.1016/j.enggeo.2018.03.014.

[66]   M. Arattano, L. Marchi, Systems and Sensors for Debris-flow Monitoring and Warning, Sensors 2008, Vol. 8, Pages 2436-2452. 8 (2008) 2436–2452. https://doi.org/10.3390/S8042436.

[67]   R.M. Iverson, The debris-flow rheology myth, (2003).

[68]   E.D. Haugen, A.M. Kaynia, Vulnerability of structures impacted by debris flow, (2008). https://doi.org/10.1201/9780203885284-c37.

[69] D. Peduto, S. Ferlisi, G. Nicodemo, D. Reale, G. Pisciotta, G. Gullà, Empirical fragility and vulnerability curves for buildings exposed to slow-moving landslides at medium and large scales, Landslides. 14 (2017) 1993–2007. https://doi.org/10.1007/S10346-017-0826-7/FIGURES/12.

[70] R.M. Iverson, Landslide triggering by rain infiltration, Water Resour Res. 36 (2000) 1897–1910. https://doi.org/10.1029/2000WR900090.

[71] O.M. Nofal, J.W. van de Lindt, T.Q. Do, Multi-variate and single-variable flood fragility and loss approaches for buildings, Reliab Eng Syst Saf. 202 (2020). https://doi.org/10.1016/j.ress.2020.106971.

[72] T. Gerl, H. Kreibich, G. Franco, D. Marechal, K. Schröter, A Review of Flood Loss Models as Basis for Harmonization and Benchmarking, PLoS One. 11 (2016) e0159791. https://doi.org/10.1371/journal.pone.0159791.

[73] D. Molinari, K.M. de Bruijn, J.T. Castillo-Rodríguez, G.T. Aronica, L.M. Bouwer, Validation of flood risk models: Current practice and possible improvements, International Journal of Disaster Risk Reduction. 33 (2019) 441–448. https://doi.org/10.1016/j.ijdrr.2018.10.022.

[74] F. Dottori, R. Figueiredo, M.L. v. Martina, D. Molinari, A.R. Scorzini, INSYDE: a synthetic, probabilistic flood damage model based on explicit cost analysis, Natural Hazards and Earth System Sciences. 16 (2016) 2577–2591. https://doi.org/10.5194/nhess-16-2577-2016.

[75] P. Deckers, W. Kellens, J. Reyns, W. Vanneuville, P. de Maeyer, A GIS for Flood Risk Management in Flanders, in: Geospatial Techniques in Urban Hazard and Disaster Analysis, Springer Netherlands, Dordrecht, 2009: pp. 51–69. https://doi.org/10.1007/978-90-481-2238-7_4.

[76] D. Sánchez-Muñoz, J.L. Domínguez-García, E. Martínez-Gomariz, B. Russo, J. Stevens, M. Pardo, Electrical Grid Risk Assessment Against Flooding in Barcelona and Bristol Cities, Sustainability. 12 (2020) 1527. https://doi.org/10.3390/su12041527.

[77] O.M. Nofal, J.W. van de Lindt, Minimal Building Flood Fragility and Loss Function Portfolio for Resilience Analysis at the Community Level, Water (Basel). 12 (2020) 2277. https://doi.org/10.3390/w12082277.

[78] M. Papathoma-Köhle, B. Gems, M. Sturm, S. Fuchs, Matrices, curves and indicators: A review of approaches to assess physical vulnerability to debris flows, Earth Sci Rev. 171 (2017) 272–288. https://doi.org/10.1016/J.EARSCIREV.2017.06.007.

[79] J.A. Prieto, M. Journeay, A.B. Acevedo, J.D. Arbelaez, M. Ulmi, Development of structural debris flow fragility curves (debris flow buildings resistance) using momentum flux rate as a hazard parameter, Eng Geol. 239 (2018) 144–157. https://doi.org/10.1016/j.enggeo.2018.03.014.

[80] F. Parisi, G. Sabella, Flow-type landslide fragility of reinforced concrete framed buildings, Eng Struct. 131 (2017) 28–43. https://doi.org/10.1016/J.ENGSTRUCT.2016.10.013.

[81] D. Asprone, F. Jalayer, A. Prota, G. Manfredi, Proposal of a probabilistic model for multi-hazard risk assessment of structures in seismic zones subjected to blast for the limit state of collapse, Structural Safety. 32 (2010) 25–34. https://doi.org/10.1016/j.strusafe.2009.04.002.

[82] M.S. Kappes, M. Keiler, K. von Elverfeldt, T. Glade, Challenges of analyzing multi-hazard risk: a review, Natural Hazards. 64 (2012) 1925–1958. https://doi.org/10.1007/s11069-012-0294-2.

[83] M.C. de Ruiter, J.A. de Bruijn, J. Englhardt, J.E. Daniell, H. de Moel, P.J. Ward, The Asynergies of Structural Disaster Risk Reduction Measures: Comparing Floods and Earthquakes, Earths Future. 9 (2021). https://doi.org/10.1029/2020EF001531.

[84] A. Mignan, S. Wiemer, D. Giardini, The quantification of low-probability–high-consequences events: part I. A generic multi-risk approach, Natural Hazards. 73 (2014) 1999–2022. https://doi.org/10.1007/s11069-014-1178-4.

[85] M.E.A. Budimir, P.M. Atkinson, H.G. Lewis, Earthquake-and-landslide events are associated with more fatalities than earthquakes alone, Natural Hazards. 72 (2014) 895–914. https://doi.org/10.1007/s11069-014-1044-4.

[86] J.C. Gill, B.D. Malamud, Reviewing and visualizing the interactions of natural hazards, Reviews of Geophysics. 52 (2014) 680–722. https://doi.org/10.1002/2013RG000445.

[87] J. Han, S. Wu, H. Wang, Preliminary Study on Geological Hazard Chains, Earth Science Frontiers. 14 (2007) 11–20. https://doi.org/10.1016/S1872-5791(08)60001-9.

[88] W. Marzocchi, A. Garcia-Aristizabal, P. Gasparini, M.L. Mastellone, A. Di Ruocco, Basic principles of multi-risk assessment: a case study in Italy, Natural Hazards. 62 (2012) 551–573. https://doi.org/10.1007/s11069-012-0092-x.

[89] S. de Angeli, B.D. Malamud, L. Rossi, F.E. Taylor, E. Trasforini, R. Rudari, A multi-hazard framework for spatial-temporal impact analysis, International Journal of Disaster Risk Reduction. 73 (2022) 102829. https://doi.org/10.1016/j.ijdrr.2022.102829.

[90] A.E. Zaghi, J.E. Padgett, M. Bruneau, M. Barbato, Y. Li, J. Mitrani-Reiser, A. McBride, Establishing Common Nomenclature, Characterizing the Problem, and Identifying Future Opportunities in Multihazard Design, Journal of Structural Engineering. 142 (2016). https://doi.org/10.1061/(ASCE)ST.1943-541X.0001586.

[91] M. Bruneau, M. Barbato, J.E. Padgett, A.E. Zaghi, J. Mitrani-Reiser, Y. Li, State of the Art of Multihazard Design, Journal of Structural Engineering. 143 (2017) 03117002. https://doi.org/10.1061/(ASCE)ST.1943-541X.0001893.

[92] H. Maiwald, J. Schwarz, Vereinheitlichte Schadensbeschreibung und Risikobewertung von Bauwerken unter extremen Naturgefahren, Bautechnik. 95 (2018) 743–755. https://doi.org/10.1002/bate.201800009.

[93] J. Schwarz, H. Maiwald, Empirical vulnerability assessment and damage description for natural hazards following the principles of modern macroseismic scales, in: 15th World Conference on Earthquake Engineering, Lisbon, Portugal, 2012. https://doi.org/10.13140/2.1.3455.4565.

[94] P.A. Korswagen, S.N. Jonkman, K.C. Terwel, Probabilistic assessment of structural damage from coupled multi-hazards, Structural Safety. 76 (2019) 135–148. https://doi.org/10.1016/j.strusafe.2018.08.001.

[95] J. Fan, Q. Li, Y. Zhang, Collapse analysis of wind turbine tower under the coupled effects of wind and near-field earthquake, Wind Energy. 22 (2019) 407–419. https://doi.org/10.1002/we.2294.

[96] K. Aljawhari, R. Gentile, F. Freddi, C. Galasso, Effects of ground-motion sequences on fragility and vulnerability of case-study reinforced concrete frames, Bulletin of Earthquake Engineering. 19 (2021) 6329–6359. https://doi.org/10.1007/s10518-020-01006-8.

[97] J.-S. Jeon, R. DesRoches, L.N. Lowes, I. Brilakis, Framework of aftershock fragility assessment-case studies: older California reinforced concrete building frames, Earthq Eng Struct Dyn. 44 (2015) 2617–2636. https://doi.org/10.1002/eqe.2599.

[98] M. Raghunandan, A.B. Liel, N. Luco, Aftershock collapse vulnerability assessment of reinforced concrete frame structures, Earthq Eng Struct Dyn. 44 (2015) 419–439. https://doi.org/10.1002/eqe.2478.

[99] S. Tesfamariam, K. Goda, G. Mondal, Seismic Vulnerability of Reinforced Concrete Frame with Unreinforced Masonry Infill Due to Main Shock–Aftershock Earthquake Sequences, Earthquake Spectra. 31 (2015) 1427–1449. https://doi.org/10.1193/042313EQS111M.

[100] L. Di Sarno, F. Pugliese, Effects of mainshock-aftershock sequences on fragility analysis of RC buildings with ageing, Eng Struct. 232 (2021) 111837. https://doi.org/10.1016/j.engstruct.2020.111837.

[101] C. Petrone, T. Rossetto, M. Baiguera, C. De la Barra Bustamante, I. Ioannou, Fragility functions for a reinforced concrete structure subjected to earthquake and tsunami in sequence, Eng Struct. 205 (2020) 110120. https://doi.org/10.1016/j.engstruct.2019.110120.

[102] G. Miluccio, R. Gentile, C. Galasso, F. Parisi, Fragility Modelling of Buildings subjected to Earthquake-Induced Landslides through Gaussian Process Regression, in: ICOSSAR 2021, International Conference on Structural Safety & Reliability, Shanghai, Cina, 2021.

[103] H. Li, Y. Liu, C. Li, X.W. Zheng, Multihazard fragility assessment of steel-concrete composite frame structures with buckling-restrained braces subjected to combined earthquake and wind, The Structural Design of Tall and Special Buildings. 29 (2020). https://doi.org/10.1002/tal.1746.

[104] X.-W. Zheng, H.-N. Li, Y.-B. Yang, G. Li, L.-S. Huo, Y. Liu, Damage risk assessment of a high-rise building against multihazard of earthquake and strong wind with recorded data, Eng Struct. 200 (2019) 109697. https://doi.org/10.1016/j.engstruct.2019.109697.

[105] D. Asprone, F. Jalayer, A. Prota, G. Manfredi, Proposal of a probabilistic model for multi-hazard risk assessment of structures in seismic zones subjected to blast for the limit state of collapse, Structural Safety. 32 (2010) 25–34. https://doi.org/10.1016/j.strusafe.2009.04.002.

[106] O.M. Nofal, J.W. van de Lindt, T.Q. Do, G. Yan, S. Hamideh, D.T. Cox, J.C. Dietrich, Methodology for Regional Multihazard Hurricane Damage and Risk Assessment, Journal of Structural Engineering. 147 (2021) 04021185. https://doi.org/10.1061/(ASCE)ST.1943-541X.0003144.

[107] H. Luo, L. Zhang, H. Wang, J. He, Multi-hazard vulnerability of buildings to debris flows, Eng Geol. 279 (2020) 105859. https://doi.org/10.1016/j.enggeo.2020.105859.

[108] G. Zuccaro, F. Cacace, R.J.S. Spence, P.J. Baxter, Impact of explosive eruption scenarios at Vesuvius, Journal of Volcanology and Geothermal Research. 178 (2008) 416–453. https://doi.org/10.1016/j.jvolgeores.2008.01.005.

[109] S.A. Argyroudis, S.A. Mitoulis, M.G. Winter, A.M. Kaynia, Fragility of transport assets exposed to multiple hazards: State-of-the-art review toward infrastructural resilience, Reliab Eng Syst Saf. 191 (2019) 106567. https://doi.org/10.1016/j.ress.2019.106567.

[110] H. Li, L. Li, G. Zhou, L. Xu, Time-dependent Seismic Fragility Assessment for Aging Highway Bridges Subject to Non-uniform Chloride-induced Corrosion, Journal of Earthquake Engineering. (2020) 1–31. https://doi.org/10.1080/13632469.2020.1809561.

[111] G. Ganesh Prasad, S. Banerjee, The Impact of Flood-Induced Scour on Seismic Fragility Characteristics of Bridges, Journal of Earthquake Engineering. 17 (2013) 803–828. https://doi.org/10.1080/13632469.2013.771593.

[112] B. Aygün, L. Dueñas-Osorio, J.E. Padgett, R. DesRoches, Efficient Longitudinal Seismic Fragility Assessment of a Multispan Continuous Steel Bridge on Liquefiable Soils, Journal of Bridge Engineering. 16 (2011) 93–107. https://doi.org/10.1061/(ASCE)BE.1943-5592.0000131.

[113] S.J. Brandenberg, P. Kashighandi, J. Zhang, Y. Huo, M. Zhao, Fragility Functions for Bridges in Liquefaction-Induced Lateral Spreads, Earthquake Spectra. 27 (2011) 683–717. https://doi.org/10.1193/1.3610248.

[114] J. Ghosh, J.E. Padgett, M. Sánchez-Silva, Seismic Damage Accumulation in Highway Bridges in Earthquake-Prone Regions, Earthquake Spectra. 31 (2015) 115–135. https://doi.org/10.1193/120812EQS347M.

[115] J.-G. Xu, G. Wu, D.-C. Feng, J.-J. Fan, Probabilistic multi-hazard fragility analysis of RC bridges under earthquake-tsunami sequential events, Eng Struct. 238 (2021) 112250. https://doi.org/10.1016/j.engstruct.2021.112250.

[116] S.A. Argyroudis, S.A. Mitoulis, M.G. Winter, A.M. Kaynia, Fragility of transport assets exposed to multiple hazards: State-of-the-art review toward infrastructural resilience, Reliab Eng Syst Saf. 191 (2019) 106567. https://doi.org/10.1016/j.ress.2019.106567.

[117] R. Gentile, S. Pampanin, C. Galasso, A computational framework for selecting the optimal combination of seismic retrofit and insurance coverage, Computer-Aided Civil and Infrastructure Engineering. in press (2021). https://doi.org/10.1111/mice.12778.

[118] D. Veneziano, A. Agarwal, E. Karaca, Decision making with epistemic uncertainty under safety constraints: An application to seismic design, Probabilistic Engineering Mechanics. 24 (2009) 426–437. https://doi.org/10.1016/j.probengmech.2008.12.004.

[119] G. Liek Yeo, A.C. Cornell, Building life-cycle cost analysis due to mainshock and aftershock occurrences, Structural Safety. 31 (2009) 396–408. https://doi.org/10.1016/j.strusafe.2009.01.002.

[120] E. Fereshtehnejad, A. Shafieezadeh, A multi-type multi-occurrence hazard lifecycle cost analysis framework for infrastructure management decision making, Eng Struct. 167 (2018) 504–517. https://doi.org/10.1016/j.engstruct.2018.04.049.

[121] V. Silva, S. Brzev, C. Scawthorn, C. Yepes, J. Dabbeek, H. Crowley, A Building Classification System for Multi-hazard Risk Assessment, International Journal of Disaster Risk Science. (2022). https://doi.org/10.1007/s13753-022-00400-x.

[122] S. Brzev, C. Scawthorn, A.W. Charleson, L. Allen, M. Greene, K. Jaiswal, V. Silva., GEM building taxonomy version 2.0. GEM Technical Report 2013-02 V1.0.0, Pavia, Italy, 2013.

[123] Applied Technology Council, Earthquake damage evaluation data for California, ATC-13., Redwood City, California, 1985.

[124] G. Grünthal, European Macroseismic Scale 1998, European Seismological Commission, Subcommission on Engineering Seismology. Working Group Macroseismic scales, 1998.

[125] FEMA (Federal Emergency Management Agency), HAZUS MH MR4 technical manual, Washington DC, USA, 2003.

[126] K.S. Jaiswal, D.J. Wald, Creating a global building inventory for earthquake loss assessment and risk management. U.S. Geological Survey Open-File Report 2008-1160., Washington DC, USA, 2008.

[127] T. Rossetto, I. Ioannou, D. Grant, Existing Empirical Fragility and Vulnerability Functions: Compendium and Guide for Selection, GEM Technical Report 2015-1, 2015. https://doi.org/10.13117.

[128] C. Galasso, M. Pregnolato, F. Parisi, A model taxonomy for flood fragility and vulnerability assessment of buildings, International Journal of Disaster Risk Reduction. 53 (2021) 101985. https://doi.org/10.1016/j.ijdrr.2020.101985.

[129] R.J. Murnane, G. Anegh, A. Busin, J. Dabbeek, H. de Moel, M. Duncan, S. Fraser, C. Galasso, C. Giovando, P. Henshaw, K. Horsburgh, C. Huyck, S. Jenkins, C. Johnson, G. Kamihanda, J. Kijazi, W. Kikwasi, W. Kombe, S. Loughlin, F. Løvholt, A. Masanja, G. Mbongoni, S. Minas, M. Msabi, M. Msechu, H. Mtongori, F. Nadim, M. O'Hara, M. Pagani, E. Phillips, T. Rossetto, R. Rudari, P. Sangana, V. Silva, J. Twigg, G. Uhinga, E. Verrucci, Data schemas for multiple hazards, exposure and vulnerability, Disaster Prevention and Management: An International Journal. 28 (2019) 752–763. https://doi.org/10.1108/DPM-09-2019-0293.

[130] C. Yepes-Estrada, V. Silva, T. Rossetto, D. D'Ayala, I. Ioannou, A. Meslem, H. Crowley, The Global Earthquake Model Physical Vulnerability Database, Earthquake Spectra. 32 (2016) 2567–2585. https://doi.org/10.1193/011816EQS015DP.

[131] H. Crowley, J. Dabbeek, V. Despotaki, D. Rodrigues, L. Martins, V. Silva, X. Romão, N. Pereira, G. Weatherill, L. Danciu, European Seismic Risk Model (ESRM20). EFEHR Technical Report 002 V1.0.0, 2021. https://doi.org/10.7414/EUC-EFEHR-TR002-ESRM20.

[132] S.P. Stefanidou, E.A. Paraskevopoulos, V.K. Papanikolaou, A.J. Kappos, An online platform for bridge-specific fragility analysis of as-built and retrofitted bridges, Bulletin of Earthquake Engineering. 20 (2022) 1717–1737. https://doi.org/10.1007/s10518-021-01299-3.

[133] M.S. Alam, B.G. Simpson, A.R. Barbosa, Defining Appropriate Fragility Functions for Oregon. A report for the Cascadia Lifelines Program (CLiP), 2020.

[134] V. Silva, H. Crowley, M. Colombi, Fragility Function Manager Tool, in: 2014: pp. 385–402. https://doi.org/10.1007/978-94-007-7872-6_13.

[135] K. Pitilakis, P. Franchin, B. Khazai, H. Wenzel, eds., SYNER-G: Systemic Seismic Vulnerability and Risk Assessment of Complex Urban, Utility, Lifeline Systems and Critical Facilities, Springer Netherlands, Dordrecht, 2014. https://doi.org/10.1007/978-94-017-8835-9.

[136] CAPRA, Integrating Disaster Risk Information Into Development Policies and Programs in Latin America and the Caribbean, 2012.

[137] I. Bombelli, D. Molinari, P. Asaridis, F. Ballio, The "Flood Damage Models" repository, in: Science and Practice for an Uncertain Future, Budapest University of Technology and Economics, Online, 2021: p. null-null. https://doi.org/10.3311/FloodRisk2020.11.3.

[138] T. Rossetto, I. Ioannou, D. Grant, Existing Empirical Fragility and Vulnerability Functions: Compendium and Guide for Selection, GEM Technical Report 2015-1, 2015. https://doi.org/10.13117.

[139] G.M. Calvi, R. Pinho, G. Magenes, J.J. Bommer, L.F. Restrepo-Velez, H. Crowley, Development of seismic vulnerability assessment methodologies over the past 30 years, Journal of Earthquake Technology. 43 (2006) 75–104.

[140] L. Martins, V. Silva, Development of a fragility and vulnerability model for global seismic risk analyses, Bulletin of Earthquake Engineering. 19 (2021) 6719–6745. https://doi.org/10.1007/s10518-020-00885-1.

[141] H. Motamed, A. Calderon, V. Silva, C. Costa, Development of a probabilistic earthquake loss model for Iran, Bulletin of Earthquake Engineering. 17 (2019) 1795–1823. https://doi.org/10.1007/s10518-018-0515-5.

[142] L. Halder, S. Chandra Dutta, R.P. Sharma, Damage study and seismic vulnerability assessment of existing masonry buildings in Northeast India, Journal of Building Engineering. 29 (2020) 101190. https://doi.org/10.1016/j.jobe.2020.101190.

[143] N. Tarque, H. Crowley, R. Pinho, H. Varum, Displacement-Based Fragility Curves for Seismic Assessment of Adobe Buildings in Cusco, Peru, Earthquake Spectra. 28 (2012) 759–794. https://doi.org/10.1193/1.4000001.

[144] B. Tang, X. Lu, L. Ye, W. Shi, Evaluation of collapse resistance of RC frame structures for Chinese schools in seismic design categories B and C, Earthquake Engineering and Engineering Vibration. 10 (2011) 369–377. https://doi.org/10.1007/s11803-011-0073-1.

[145] N. Ahmad, A. Shahzad, Q. Ali, M. Rizwan, A.N. Khan, Seismic fragility functions for code compliant and non-compliant RC SMRF structures in Pakistan, Bulletin of Earthquake Engineering. 16 (2018) 4675–4703. https://doi.org/10.1007/s10518-018-0377-x.

[146] J. Huizinga, H. de Moel, W. Szewczyk, Global flood depth-damage functions: methodology and the database with guidelines, EUR 28552 EN, Ispra, Italy, 2017. https://doi/https://doi. org/10.2760/16510.

[147] J. Dabbeek, V. Silva, C. Galasso, A. Smith, Probabilistic earthquake and flood loss assessment in the Middle East, International Journal of Disaster Risk Reduction. 49 (2020) 101662. https://doi.org/10.1016/J.IJDRR.2020.101662.

[148] K. Porter, GEM Vulnerability Rating System, GEM Global Vulnerability Estimation Methods Consortium, 2011.

[149] A. Meslem, D. D'Ayala, I. Ioannu, T. Rossetto, D. Lang, Uncertainty and Quality Rating in Analytical Vulnerability Assessment, in: Second European Conference on Earthquake Engineering and Seismology, Istanbul, Turkey, 2014.

[150] T. Rossetto, D. D'Ayala, I. Ioannou, A. Meslem, Evaluation of Existing Fragility Curves, in: 2014: pp. 47–93. https://doi.org/10.1007/978-94-007-7872-6_3.

[151] T.L. Saaty, The analytical hierarchy process, McGraw-Hill, New York, USA, 1980.

[152] R. Gentile, C. Galasso, Simplified seismic loss assessment for optimal structural retrofit of RC buildings [Open Access], Earthquake Spectra. 37 (2020). https://doi.org/10.1177/8755293020952441.

[153] C.L. (Ching-L. Hwang, Kwangsun. Yoon, Multiple Attribute Decision Making : Methods and Applications A State-of-the-Art Survey, Springer Berlin Heidelberg, 1981.

[154] N. Caterino, I. Iervolino, G. Manfredi, E. Cosenza, Comparative analysis of multi-criteria decision-making methods for seismic structural retrofitting, Computer-Aided Civil and Infrastructure Engineering. 24 (2009) 432–445. https://doi.org/10.1111/j.1467-8667.2009.00599.x.

[155] A. Afsordegan, M. Sánchez, N. Agell, S. Zahedi, L. v. Cremades, Decision making under uncertainty using a qualitative TOPSIS method for selecting sustainable energy alternatives, International Journal of Environmental Science and Technology. 13 (2016) 1419–1432. https://doi.org/10.1007/s13762-016-0982-7.

[156] J. Baker, Probabilistic Seismic Hazard Analysis, 2.0.1, 2013.

[157] D. D'Ayala, A. Meslem, D. Vamvatsikos, K. Porter, T. Rossetto, H. Crowley, V. Silva, Guidelines for Analytical Vulnerability Assessment - Low/Mid-Rise, GEM Technical Report. (2013). https://doi.org/10.13117/GEM.VULN-MOD.TR2014.12.

[158] O.O. Thomas, L. Chouinard, S. Langlois, Probabilistic Fatigue Fragility Curves for Overhead Transmission Line Conductor-Clamp Assemblies, Front Built Environ. 8 (2022). https://doi.org/10.3389/fbuil.2022.833167.

[159] R. Gentile, C. Galasso, Hysteretic energy-based state-dependent fragility for ground-motion sequences, Earthq Eng Struct Dyn. 50 (2021) 1187–1203. https://doi.org/10.1002/eqe.3387.

[160] Federal Emergency Management Agency, Seismic Performance Assessment of Buildings. Volume 1 - Methodology, Washington, DC, 2012.

[161] O.M. Nofal, J.W. van de Lindt, Minimal building flood fragility and loss function portfolio for resilience analysis at the community level, Water (Switzerland). 12 (2020). https://doi.org/10.3390/w12082277.

[162] N.C. Dalkey, The Delphi Method: An Experimental Study of Group Opinion, Santa Monica, USA, 1969.

[163] K. Porter, A Beginner's Guide to Fragility, Vulnerability, and Risk, 2021.

[164] K. Porter, R. Kennedy, R. Bachman, Creating fragility functions for performance-based earthquake engineering, Earthquake Spectra. 23 (2007) 471–489. https://doi.org/10.1193/1.2720892.

[165] J.W. Baker, Efficient analytical fragility function fitting using dynamic structural analysis, Earthquake Spectra. 31 (2015) 579–599. https://doi.org/10.1193/021113EQS025M.

[166] F. Jalayer, Direct Probabilistic Seismic Analysis: Implementation Non-Linear Dynamic Assessments, Stanford University, 2003.

[167] D. Vamvatsikos, A.C. Cornell, Incremental dynamic analysis, Earthq Eng Struct Dyn. 31 (2002) 491–514. https://doi.org/10.1002/EQE.141.

[168] M. Kohrangi, D. Vamvatsikos, P. Bazzurro, Site dependence and record selection schemes for building fragility and regional loss assessment, Earthq Eng Struct Dyn. 46 (2017) 1625–1643. https://doi.org/10.1002/eqe.2873.

[169] G. Cremen, E.Y. Mentese, M.E. Filippi, R. Gentile, C. Galasso, J. McCloskey, A State-of-the-Art Environment for Supporting Risk-Sensitive Decisions on Urbanisation in Tomorrow's Cities, International Journal of Disaster Risk Reduction. under rev (2022).

[170] L. Jenkins, M. Creed, K. Tarbali, M. Muthusamy, robert sakic Trogrlic, J. Philips, S. Watson, H. Sinclair, C. Galasso, J. McCloskey, Physics-based simulations of multiple natural hazards for risk sensitive land use planning in expanding urban regions undefined, International Journal of Disaster Risk Reduction. under rev (2022).

[171] E.Y. Mentese, G. Cremen, R. Gentile, M.E. Filippi, C. Galasso, J. McCloskey, Risk-Informed Urbanisation Scenario Development through Interdisciplinary and GIS-Based Processes, International Journal of Disaster Risk Reduction. under rev (2022).

[172] E.Y. Mentese, G. Cremen, R. Gentile, M.L. Filippi, C. Galasso, J. McCloskey, Risk-informed Urbanisation Scenario Development through Interdisciplinary and GIS-Based Processes, International Journal of Disaster Risk Reduction. under rev (2022).

[173] NBC: 201, Nepal national building code, Kathmandu, Nepal, 1994.

[174] S. Akkar, H. Sucuoğlu, A. Yakut, Displacement-Based Fragility Functions for Low- and Mid-rise Ordinary Concrete Buildings, Earthquake Spectra. 21 (2005) 901–927. https://doi.org/10.1193/1.2084232.

[175] M.A. Erberik, Fragility-based assessment of typical mid-rise and low-rise RC buildings in Turkey, Eng Struct. 30 (2008) 1360–1374. https://doi.org/10.1016/j.engstruct.2007.07.016.

[176] G. Sevieri, C. Galasso, D. D'Ayala, R. de Jesus, A. Oreta, M.E.D.A. Grio, R. Ibabao, A multi-hazard risk prioritisation framework for cultural heritage assets, Natural Hazards and Earth System Sciences. 20 (2020) 1391–1414. https://doi.org/https://doi.org/10.5194/nhess-20-1391-2020.

[177] R. Gentile, C. Galasso, Y. Idris, I. Rusydy, E. Meilianda, From rapid visual survey to multi-hazard risk prioritisation and numerical fragility of school buildings in Banda Aceh, Indonesia, Natural Hazards and Earth System Sciences. 19 (2019) 1365–1386. https://doi.org/10.5194/nhess-2018-397.

[178] D. Gautam, G. Fabbrocino, F. Santucci de Magistris, Derive empirical fragility functions for Nepali residential buildings, Eng Struct. 171 (2018) 617–628. https://doi.org/10.1016/j.engstruct.2018.06.018.

[179] R. Gentile, C. Galasso, Simplicity versus accuracy trade-off in estimating seismic fragility of existing reinforced concrete buildings, Soil Dynamics and Earthquake Engineering. 144 (2021) 106678. https://doi.org/10.1016/j.soildyn.2021.106678.

[180] J.C.S. Tang, S. Vongvisessomjai, K. Sahasakmontri, Estimation of flood damage cost for Bangkok, Water Resources Management. 6 (1992) 47–56. https://doi.org/10.1007/BF00872187.

[181] R. Guragain, Development of seismic risk assessment system for Nepal, University of Tokyo, 2015. https://doi.org/http://doi.org/10.15083/00007589.

[182] R. Gentile, C. Galasso, Simplicity versus accuracy trade-off in estimating seismic fragility of existing reinforced concrete buildings, Soil Dynamics and Earthquake Engineering. 144 (2021) 106678. https://doi.org/10.1016/j.soildyn.2021.106678.
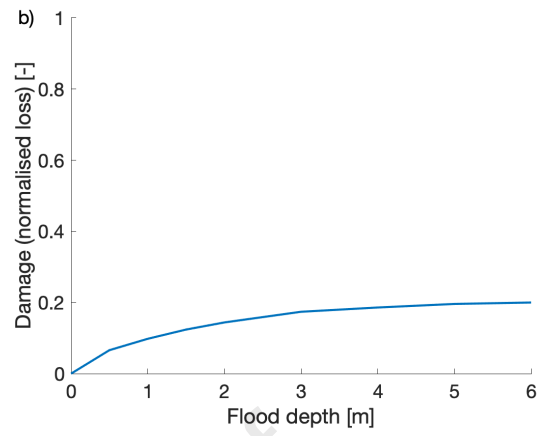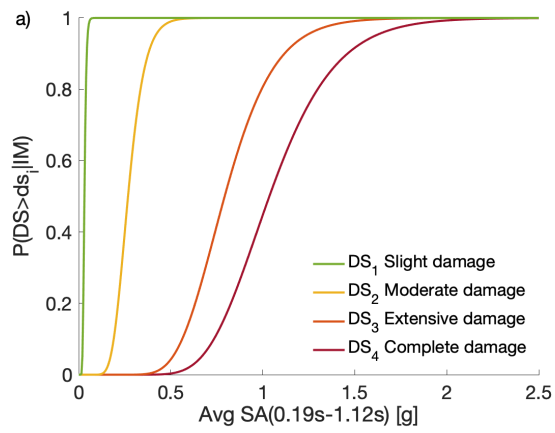
Declaration of interests

☐ The authors declare that they have no known competing financial interests or personal relationships that could have appeared to influence the work reported in this paper.

☒ The authors declare the following financial interests/personal relationships which may be considered as potential competing interests:

All authors reports financial support was provided by UK Research and Innovation.